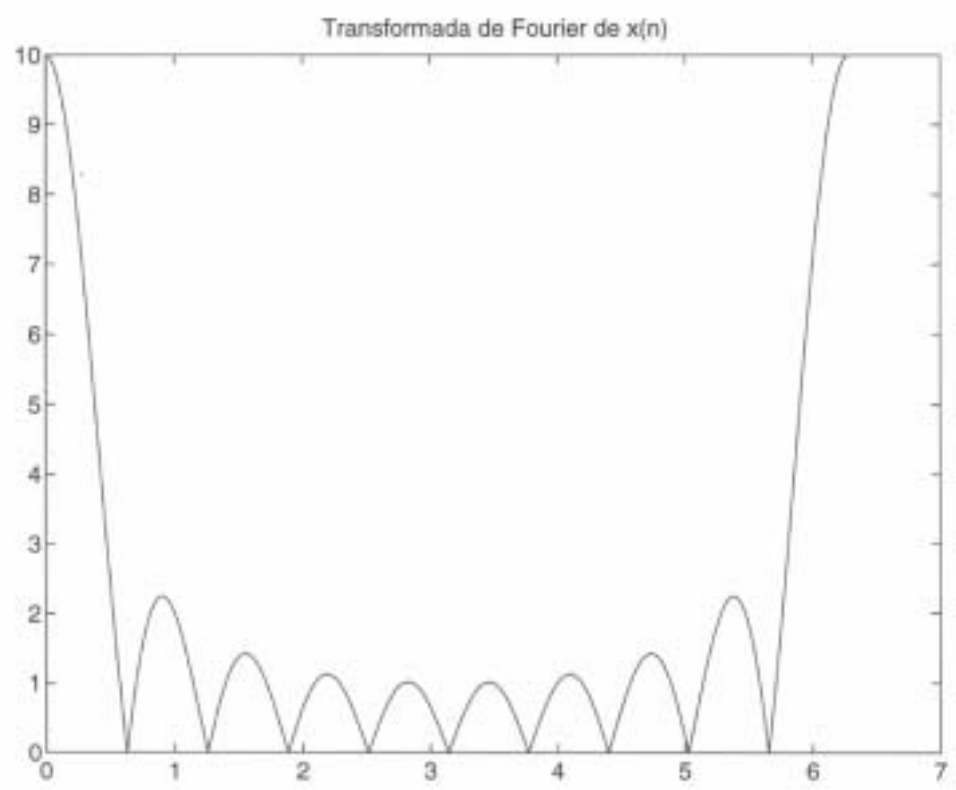
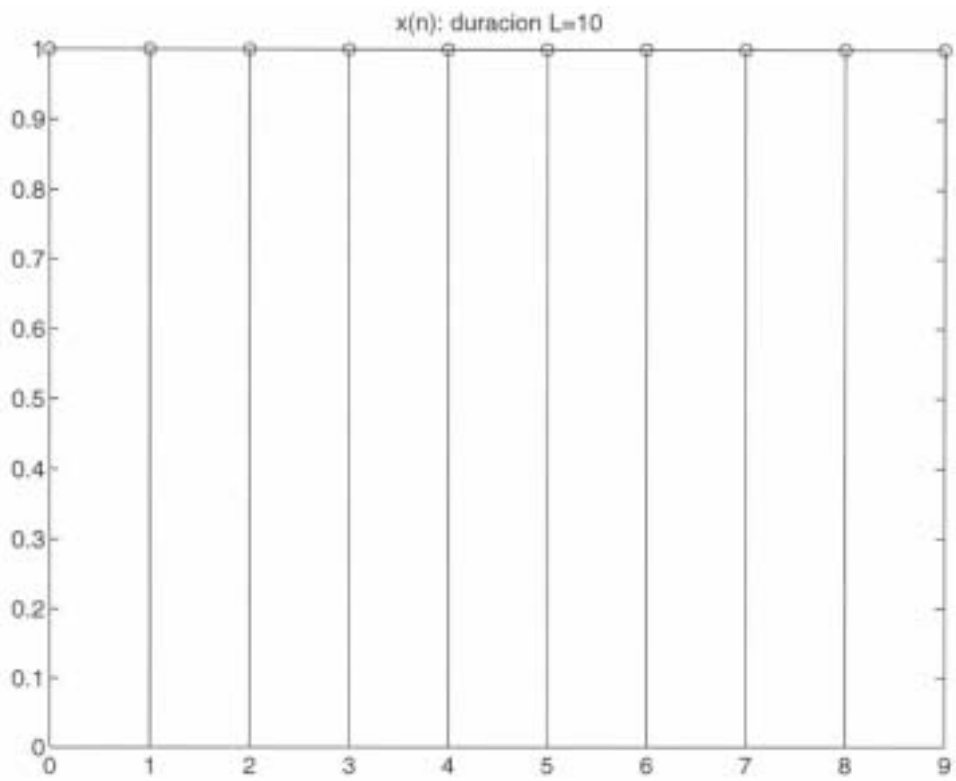
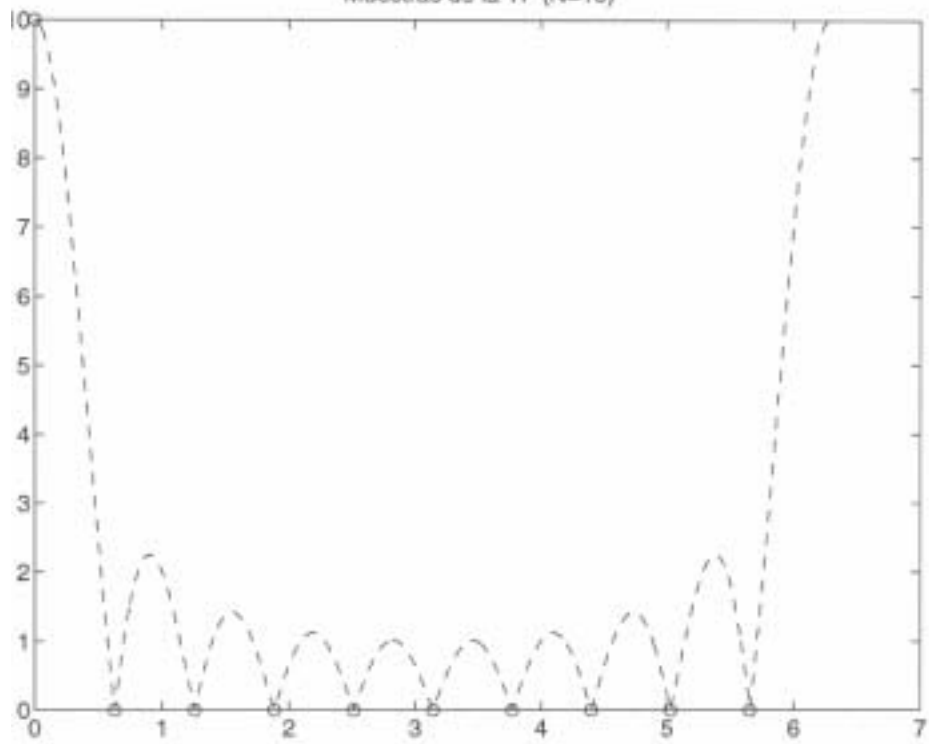


Tratamiento Digital de la Señal

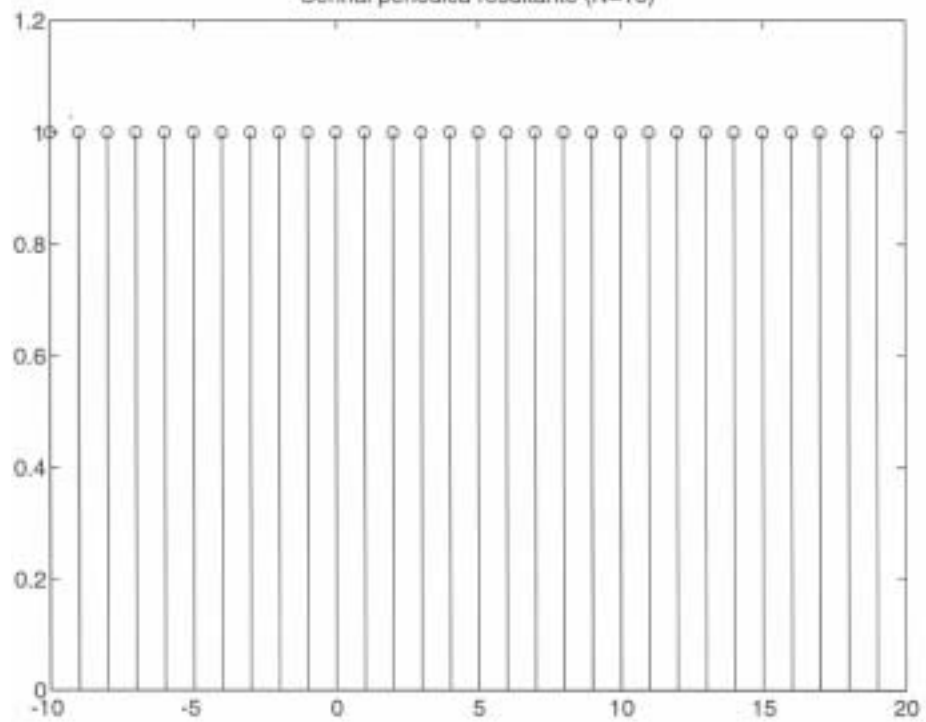
Tema 3

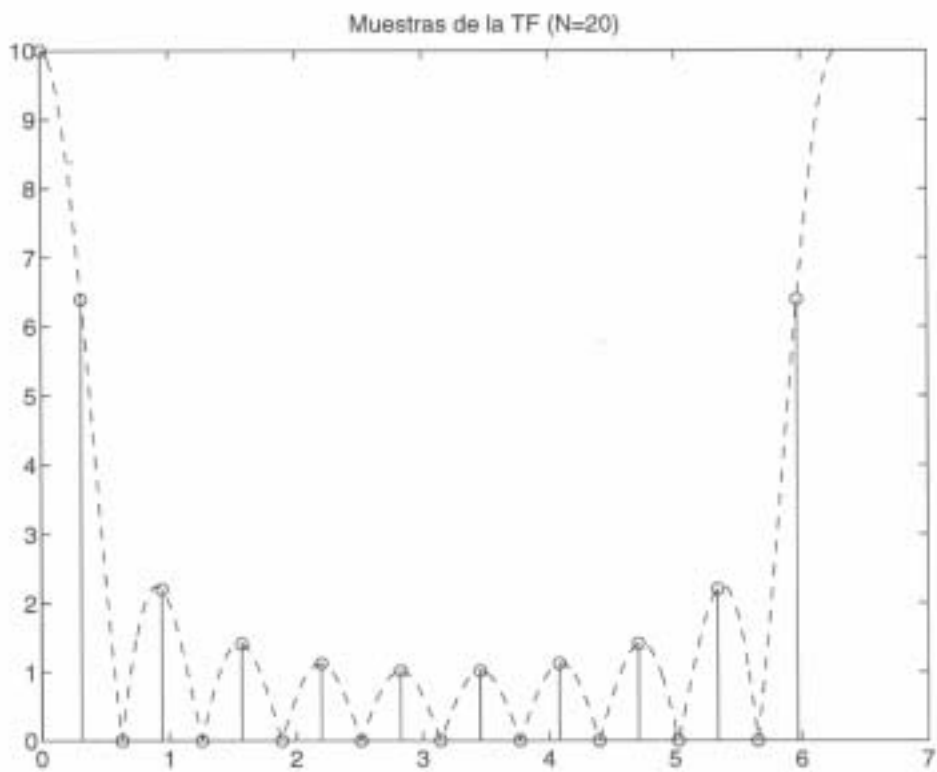
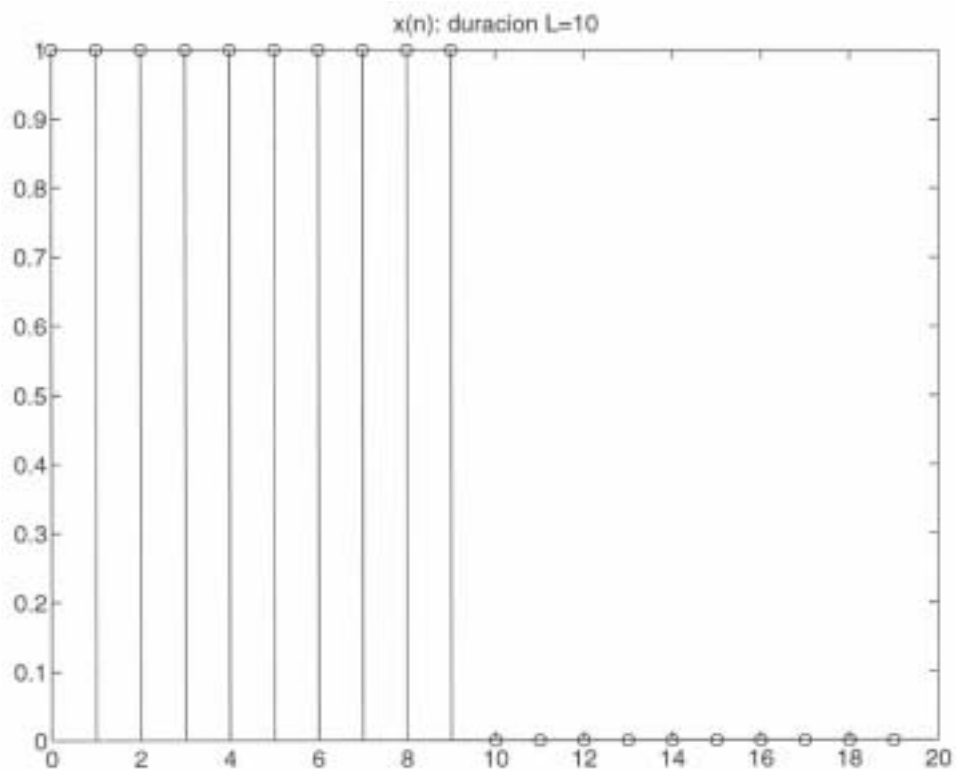


Muestras de la TF (N=10)

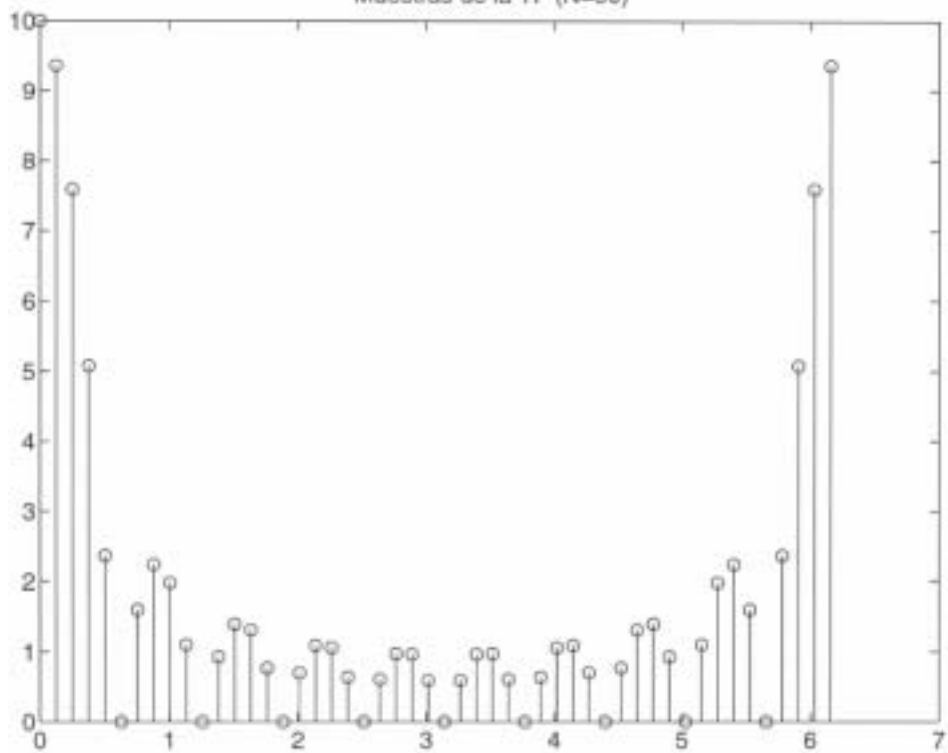


Señal periodica resultante (N=10)

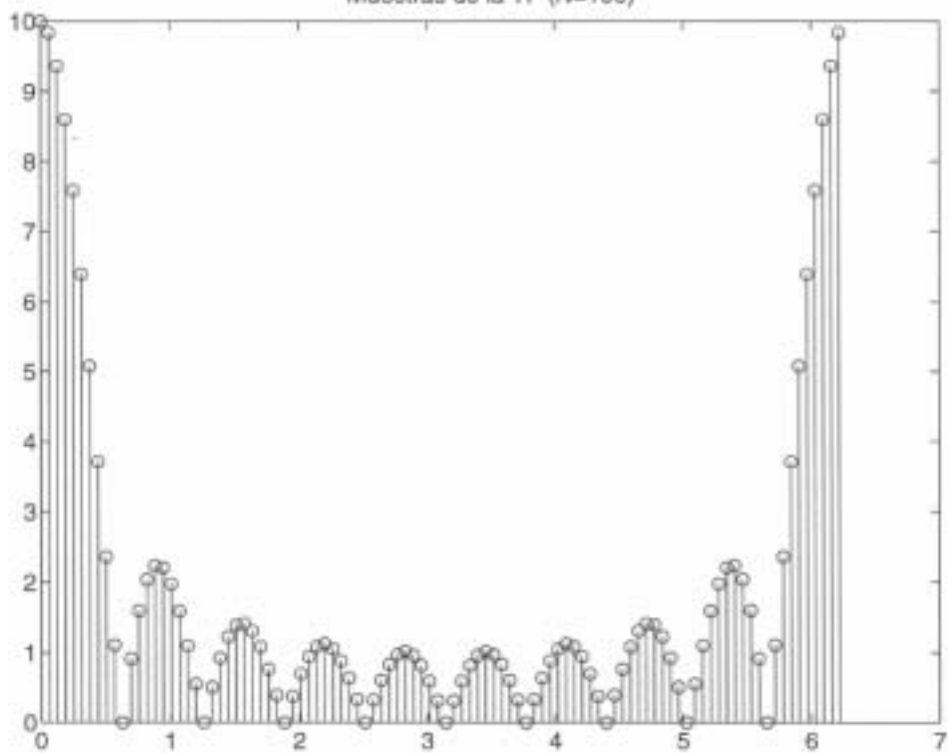




Muestras de la TF (N=50)



Muestras de la TF (N=100)



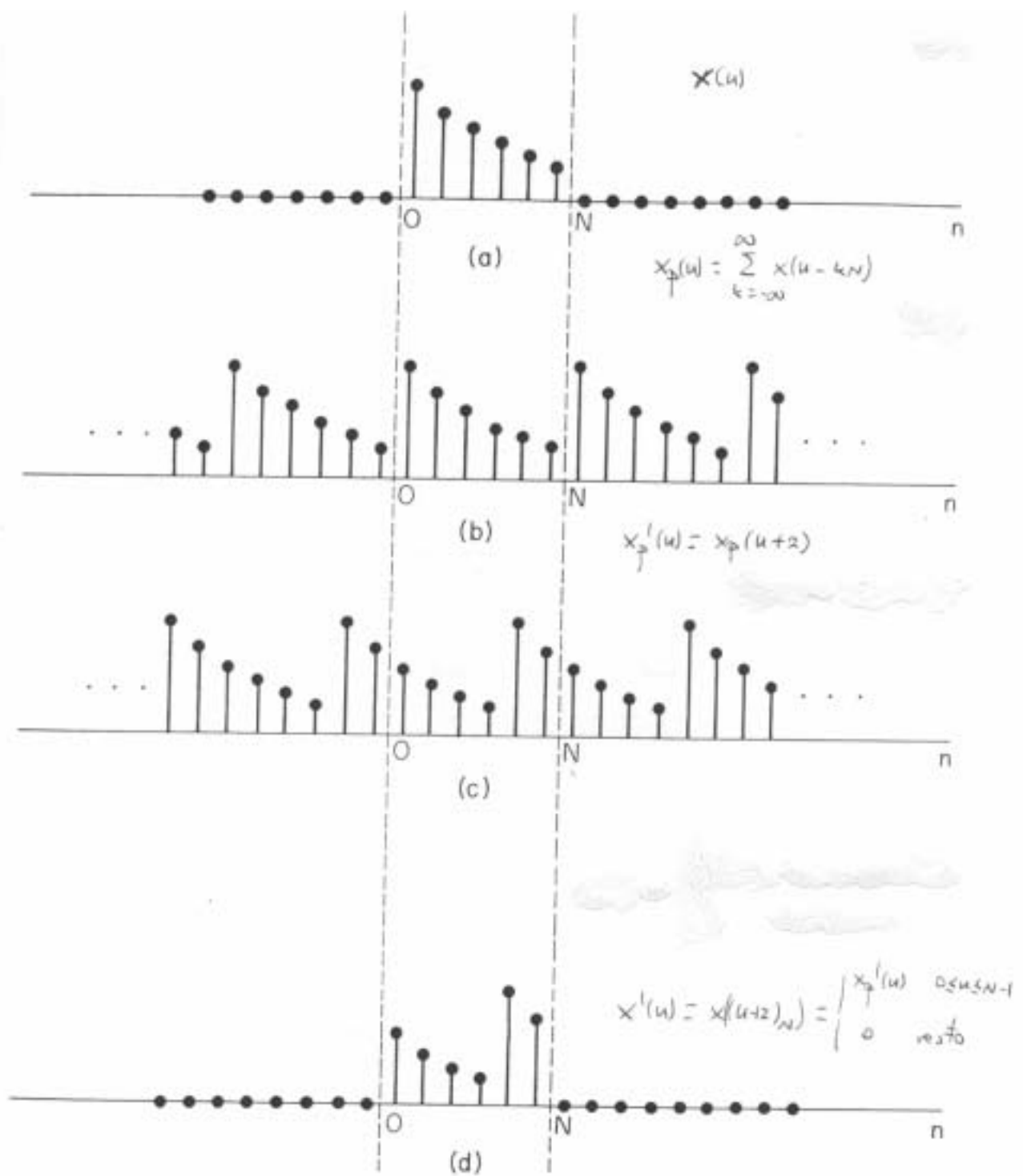
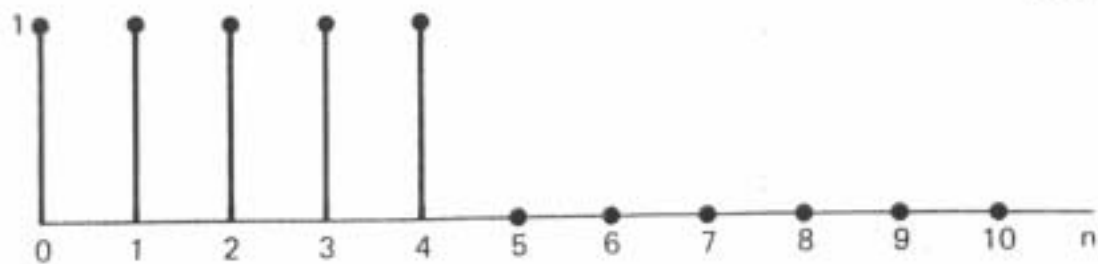
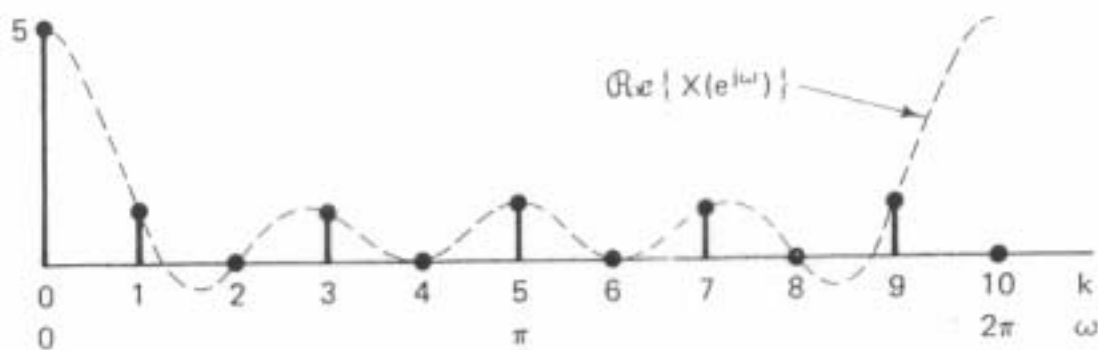


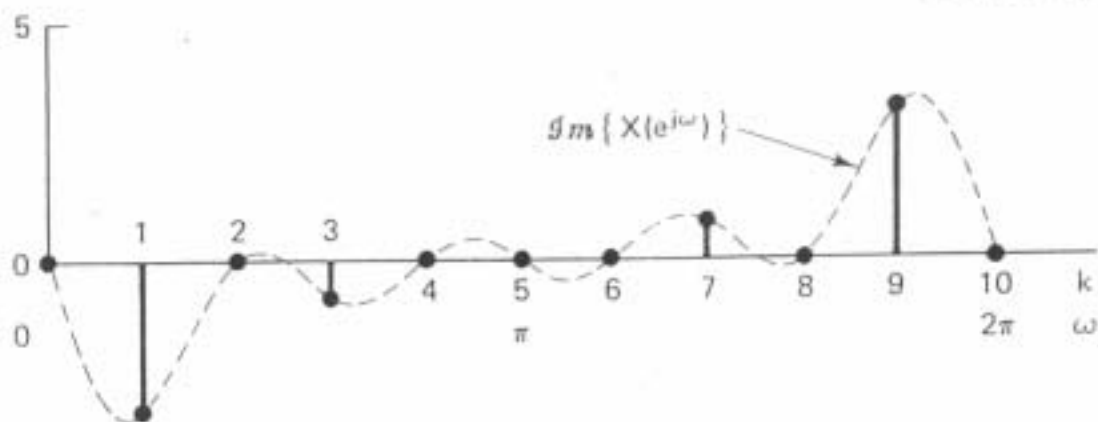
Figure 8.12 Circular shift of a finite-length sequence; i.e., the effect in the time domain of multiplying the DFT of the sequence by a linear phase shift.

$x[n]$ 

(a)

 $\Re\{X[k]\}$ 

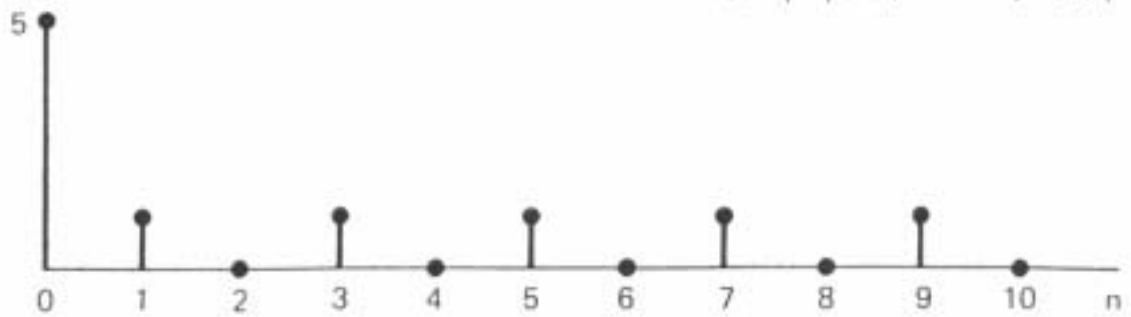
(b)

 $\Im\{X[k]\}$ 

(c)

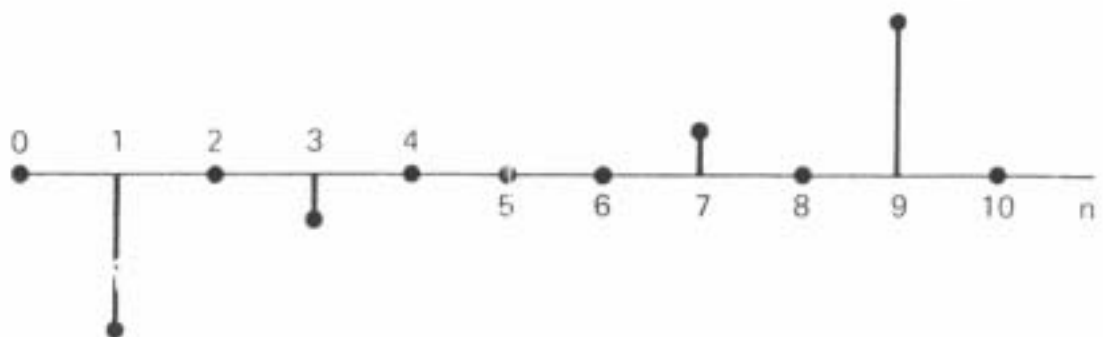
Figure 8.13 (continued) (d) and (e) The real and imaginary parts of the dual sequence $x_1[n] = X[n]$. (f) The DFT of $x_1[n]$.

$$\Re\{x_1[n]\} = \Re\{X[n]\}$$



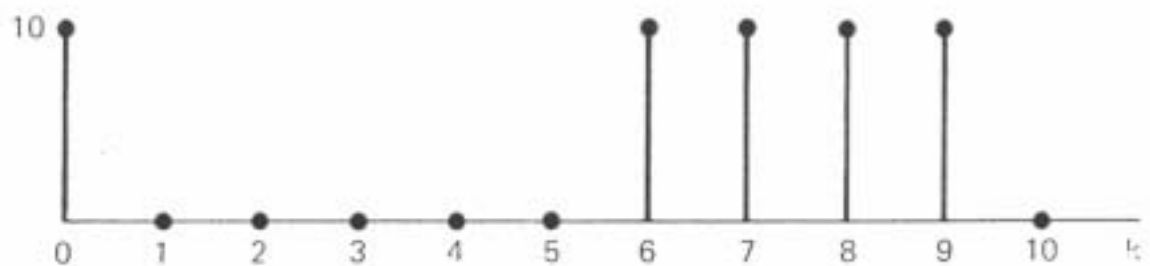
(d)

$$\Im\{x_1[n]\} = \Im\{X[n]\}$$



(e)

$$X_1[k] = 10 \times [((-k))_{10}]$$



(f)

Figure 8.13 (continued) (d) and (e) The real and imaginary parts of the dual sequence $x_1[n] = X[n]$. (f) The DFT of $x_1[n]$.

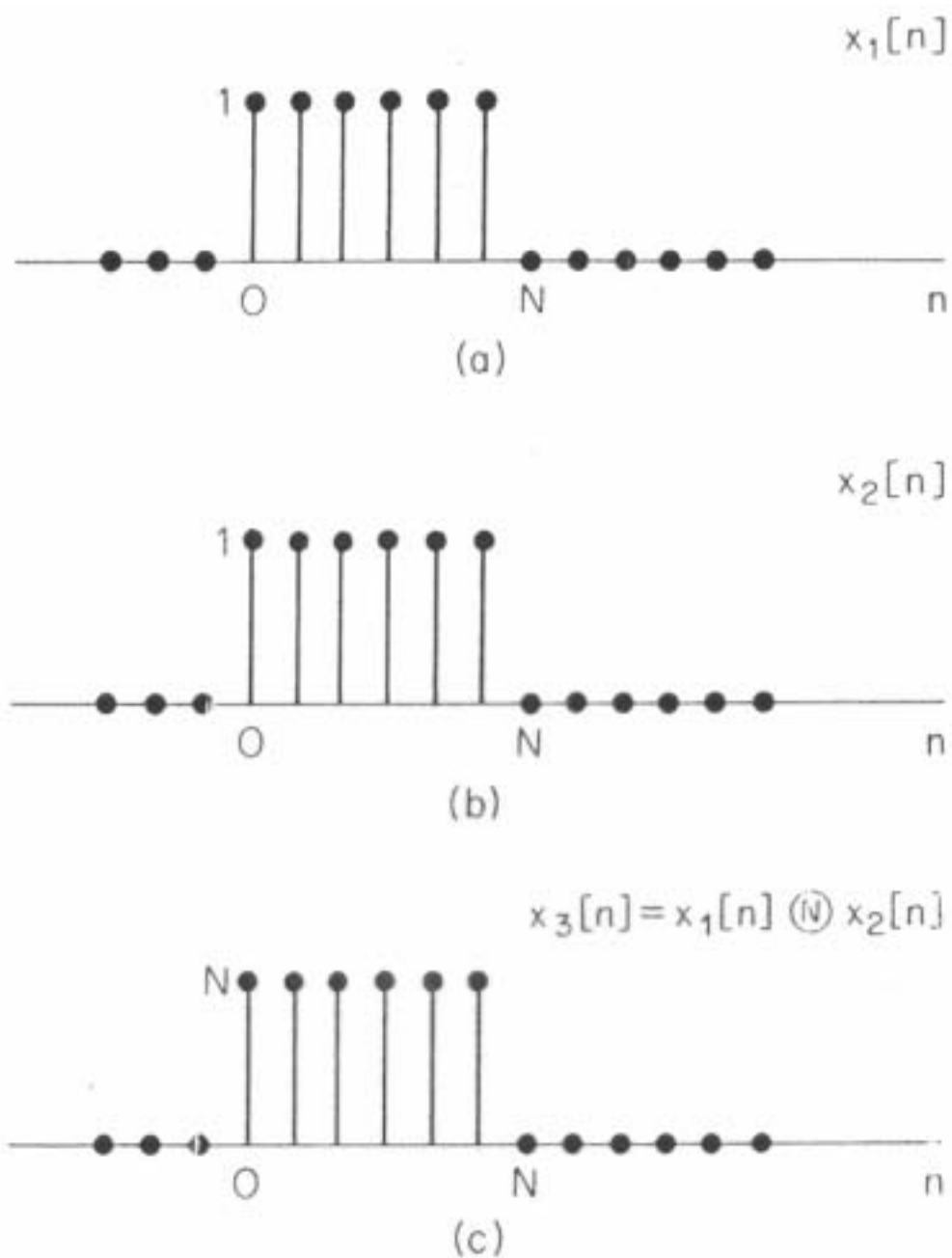


Figure 8.15 N -point circular convolution of two constant sequences of length N .

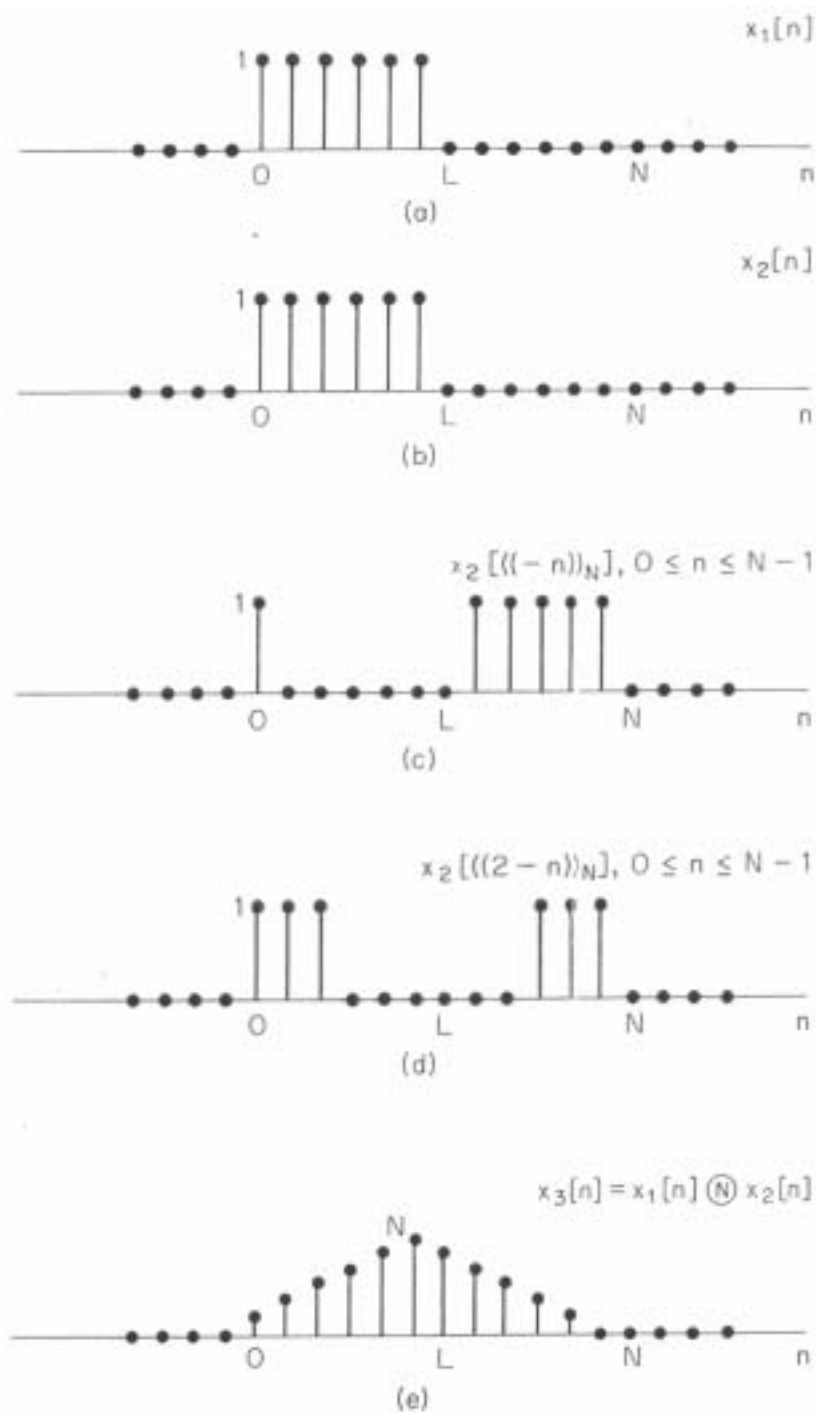
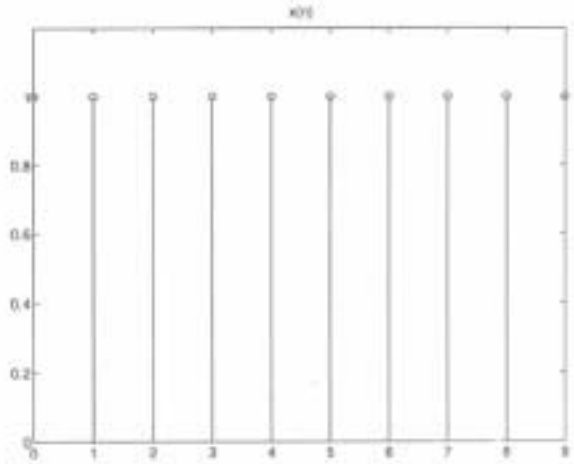
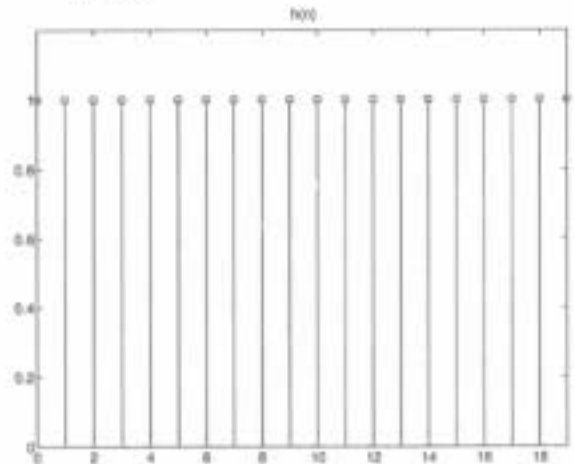


Figure 8.16 $2L$ -point circular convolution of two constant sequences of length L .

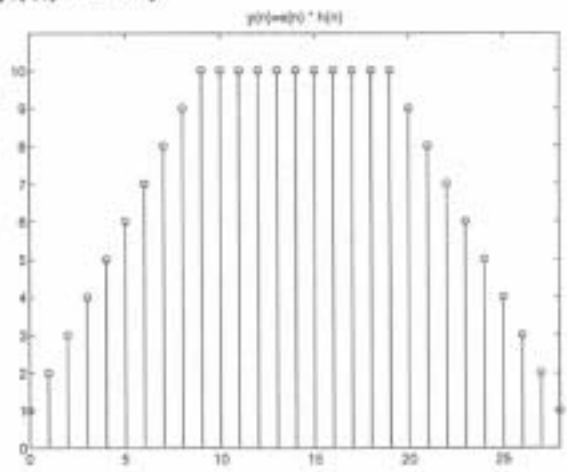
$x(n)$



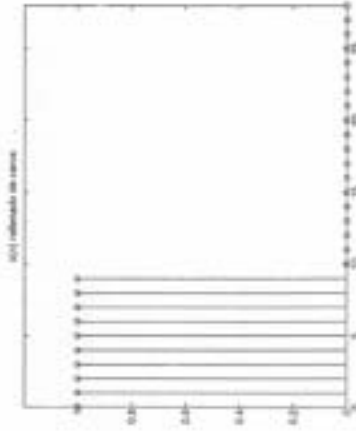
$h(n)$



$y(n) = x(n) * h(n)$

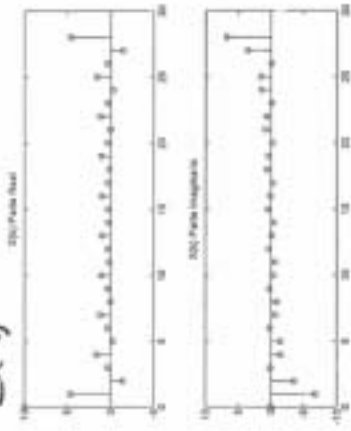


$x(n)$

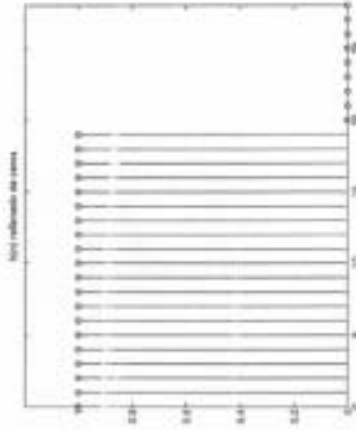


$\mathcal{D}\pm\mathcal{T}$

$X(z)$

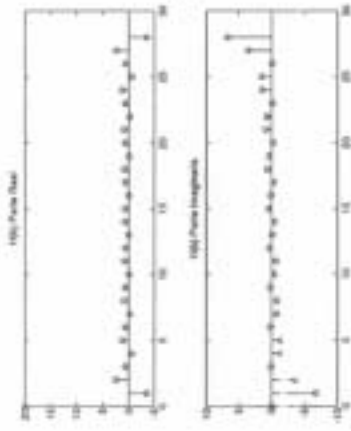


$h(n)$

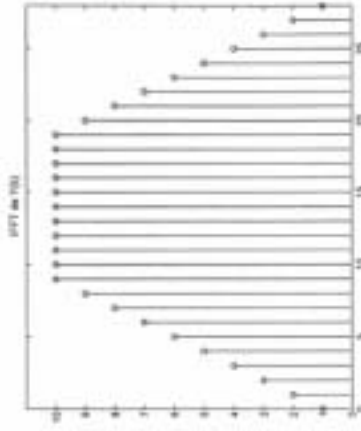


$\mathcal{D}\pm\mathcal{T}$

$H(z)$

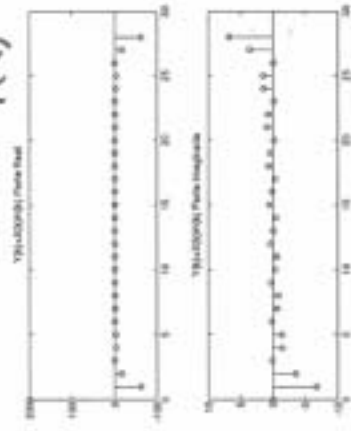


$y(n)$



$\mathcal{D}\pm\mathcal{T}$

$Y(z)$



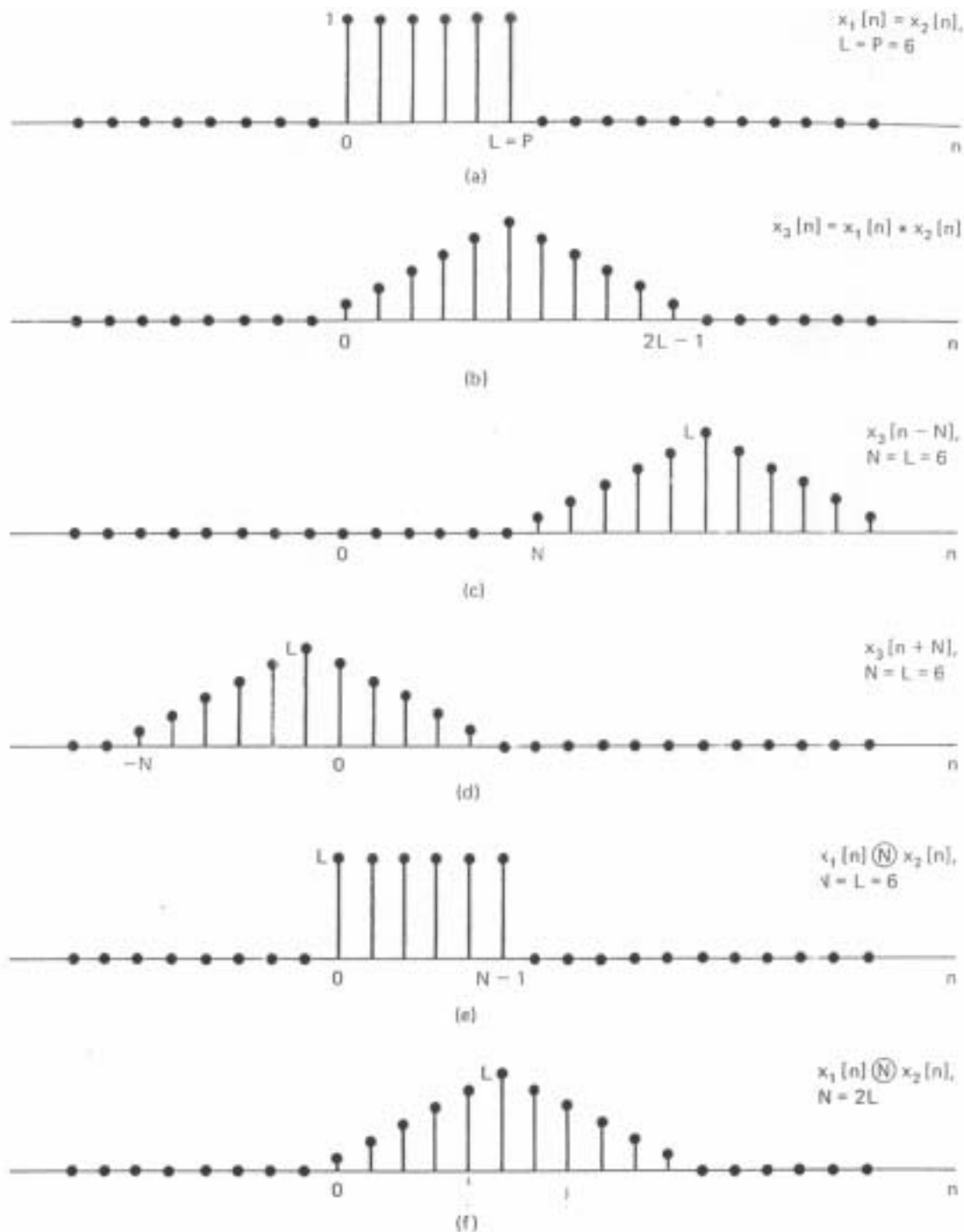
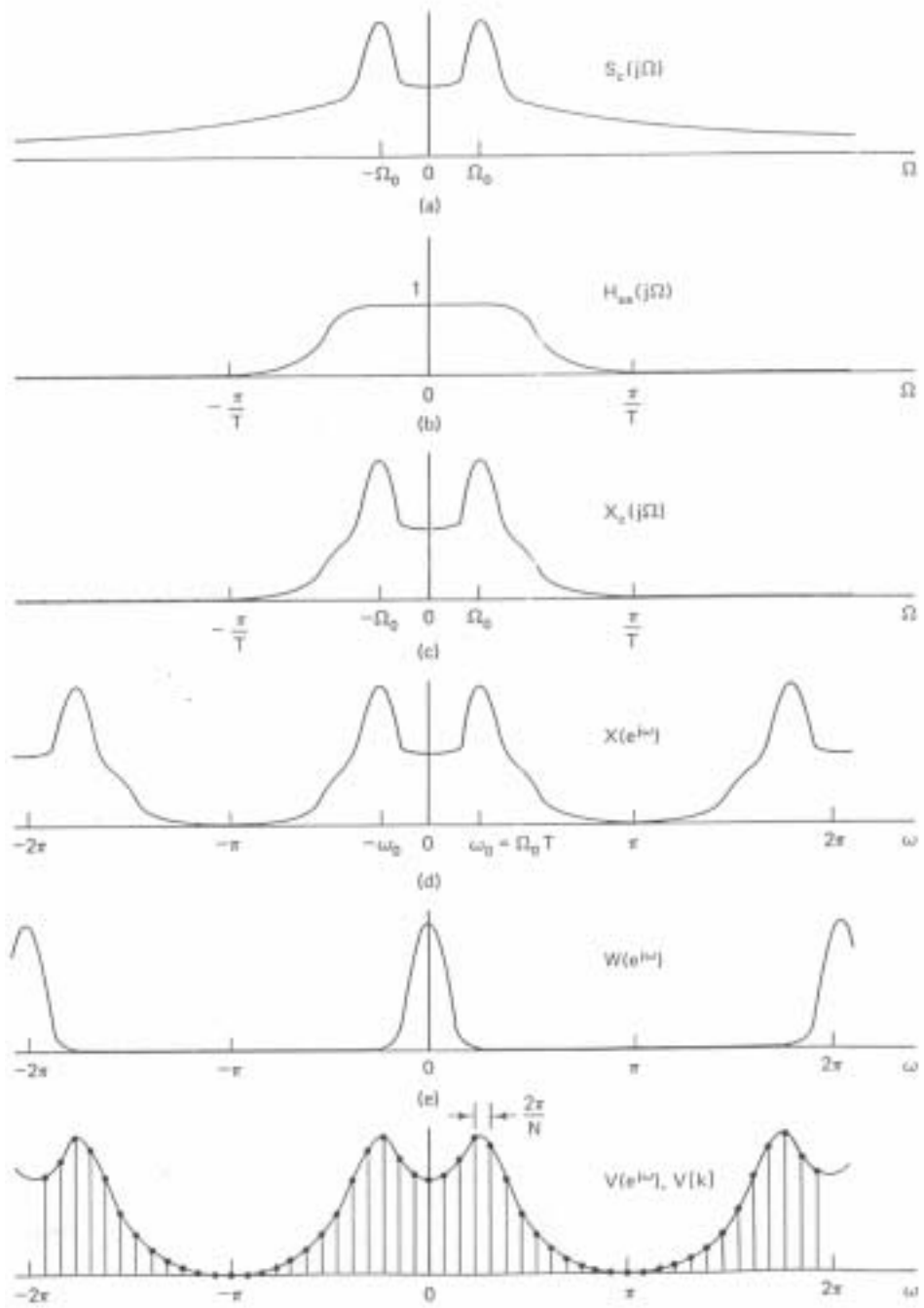


Figure 8.18 Illustration that circular convolution is equivalent to linear convolution followed by aliasing. (a) The sequences $x_1[n]$ and $x_2[n]$ to be convolved. (b) The linear convolution of $x_1[n]$ and $x_2[n]$. (c) $x_3[n - N]$ for $N = 6$. (d) $x_3[n + N]$ for $N = 6$. (e) $x_1[n] \otimes x_2[n]$, which is equal to the sum of (b), (c), and (d) in the interval $0 \leq n \leq 5$. (f) $x_1[n] \otimes x_2[n]$.

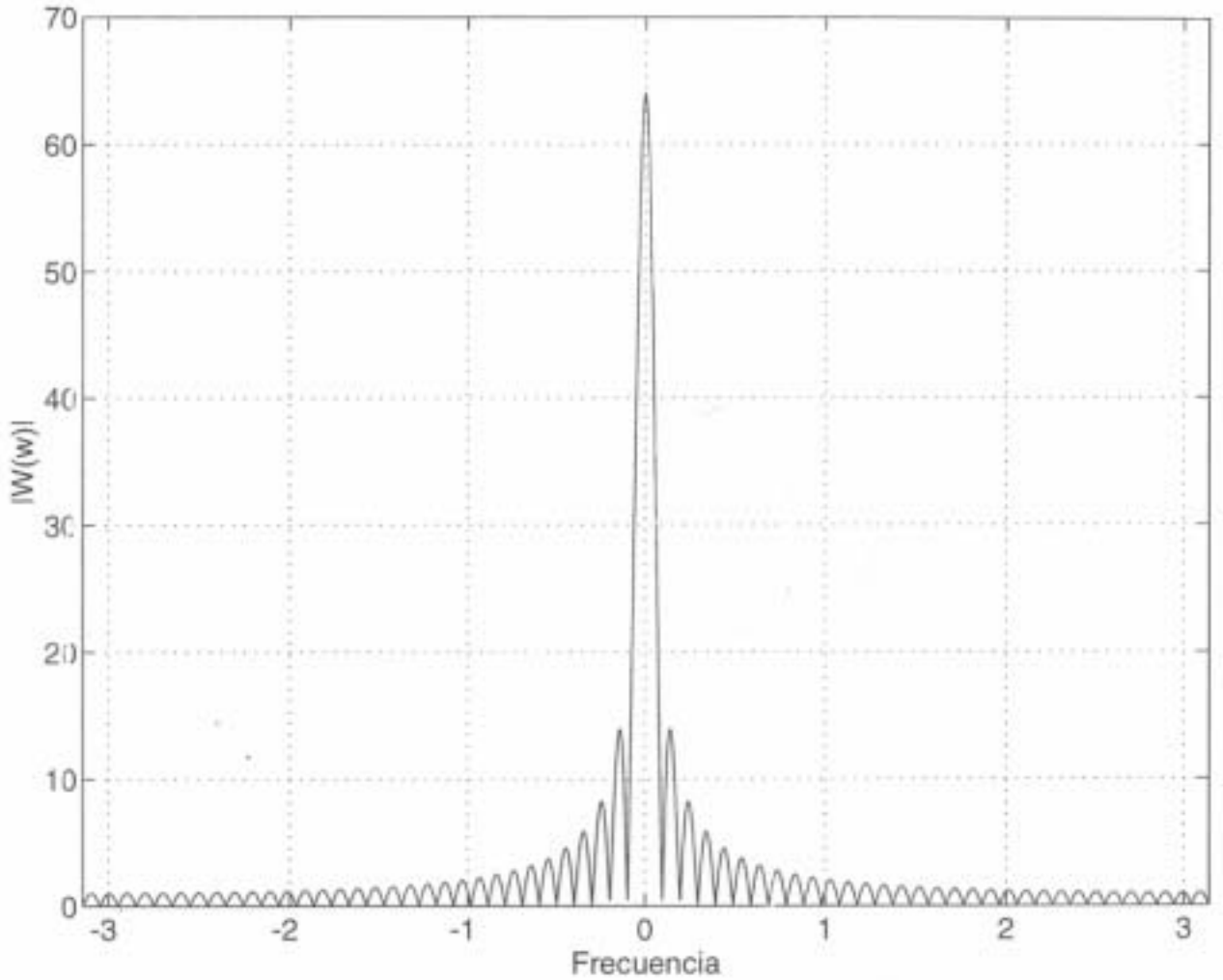


Figure 11.1 Processing steps in the discrete-time Fourier analysis of a continuous-time signal.

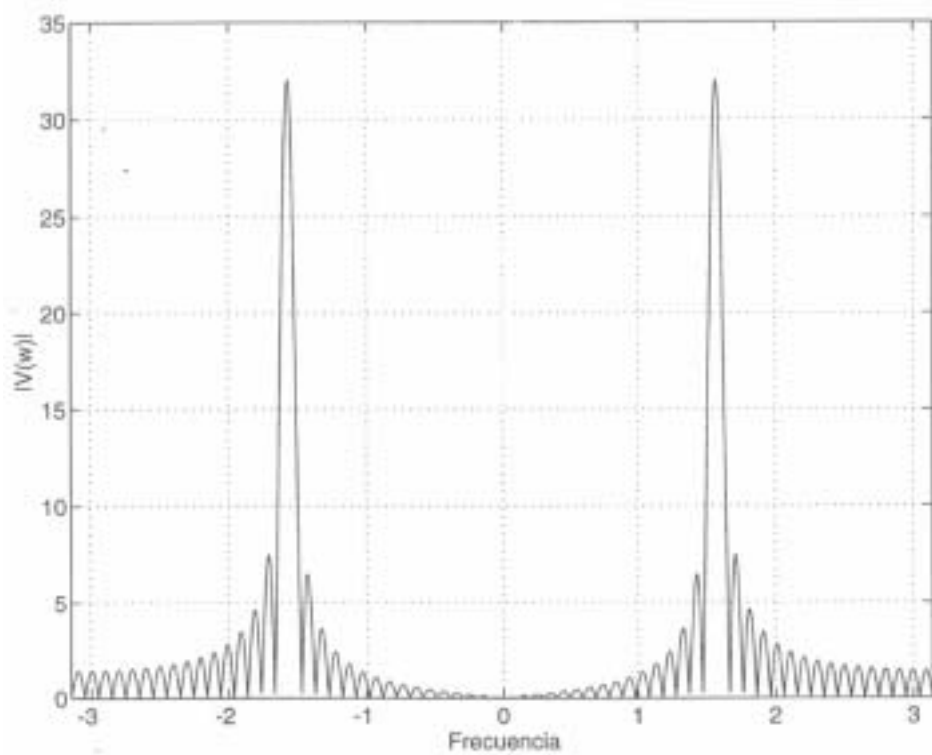
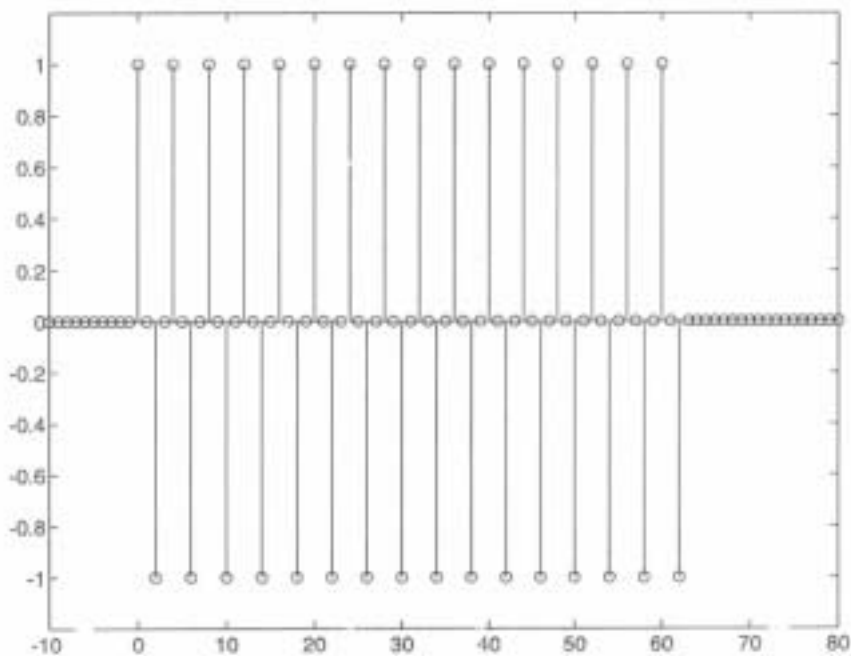


Ventana Rectangular L=64

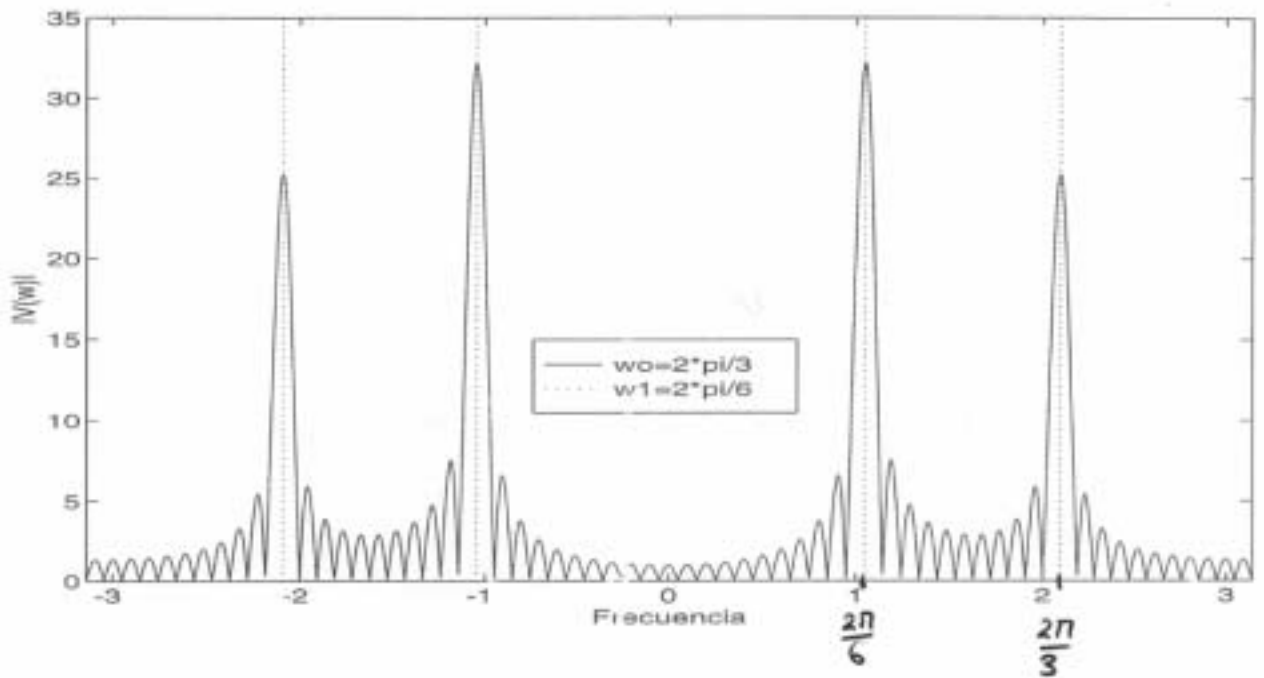
$$|W(e^{j\omega})| = \frac{\text{sen}(\omega L/2)}{\text{sen}(\omega/2)}$$



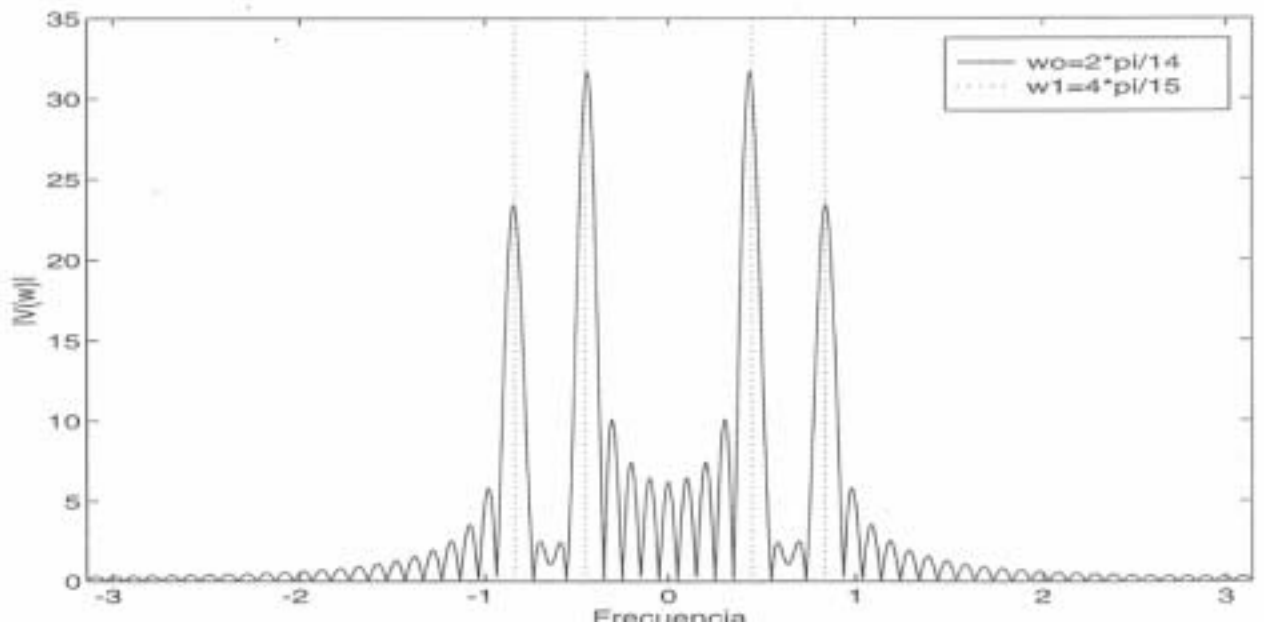
$$x(n) = \cos\left(\frac{\pi}{2}n\right) \quad n = 0, \dots, 63$$



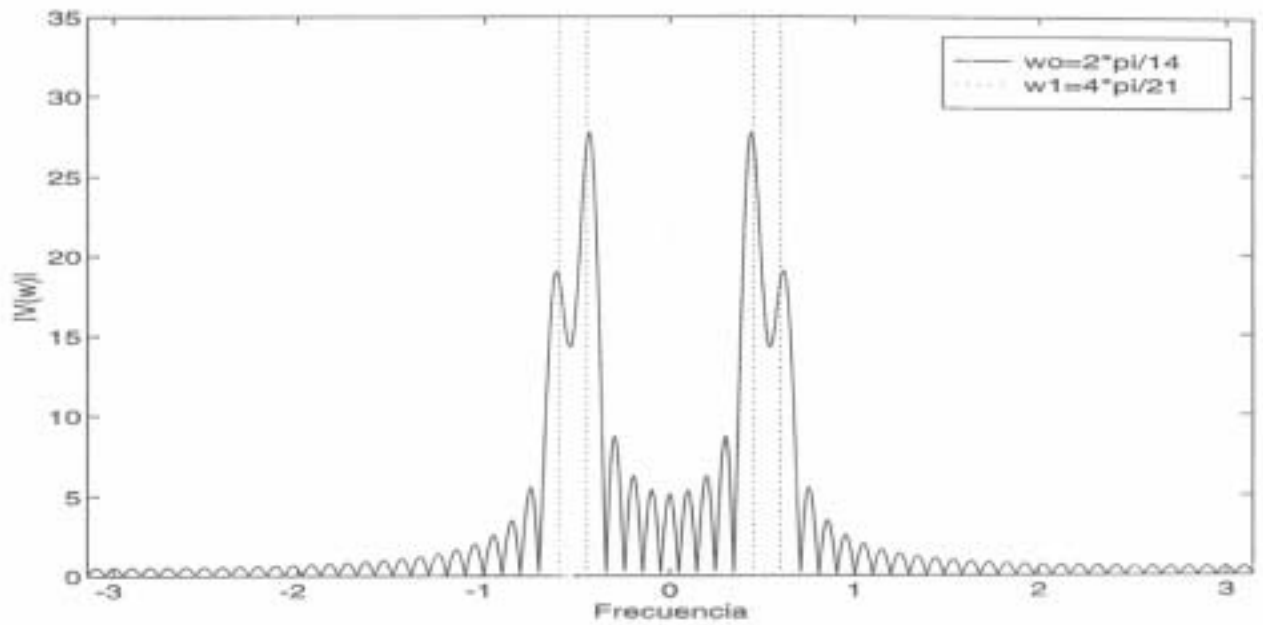
$$\omega_0 = \frac{2\pi}{3} \quad \omega_1 = \frac{2\pi}{6}$$



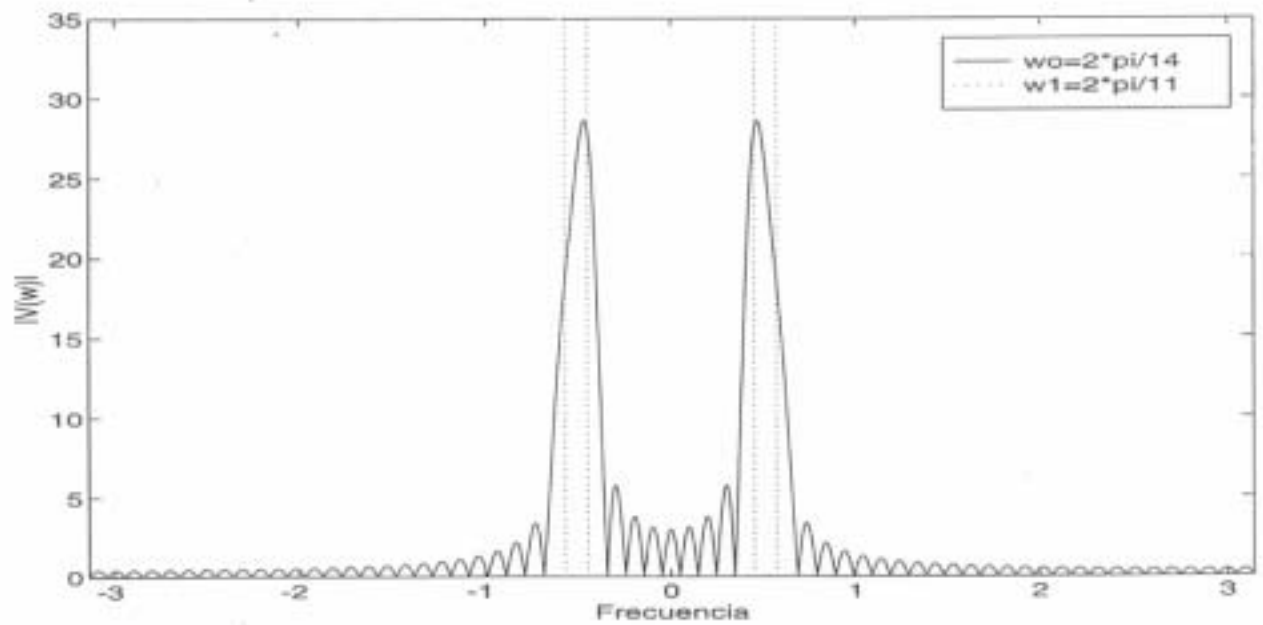
$$\omega_0 = \frac{2\pi}{14} \quad \omega_1 = \frac{4\pi}{15}$$



$$\omega_0 = \frac{2\pi}{14} \quad \omega_1 = \frac{4\pi}{21}$$

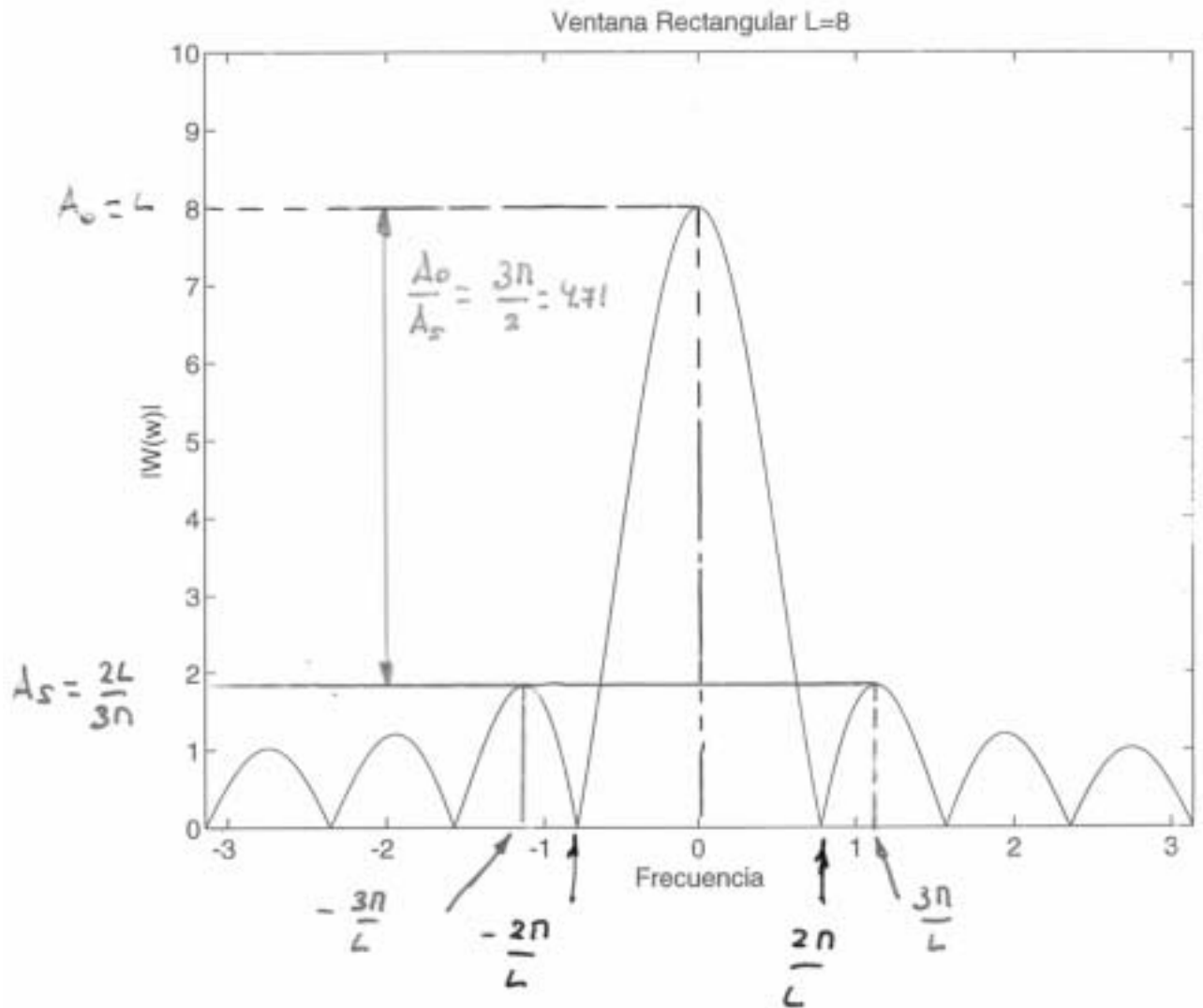


$$\omega_0 = \frac{2\pi}{14} \quad \omega_1 = \frac{2\pi}{11}$$

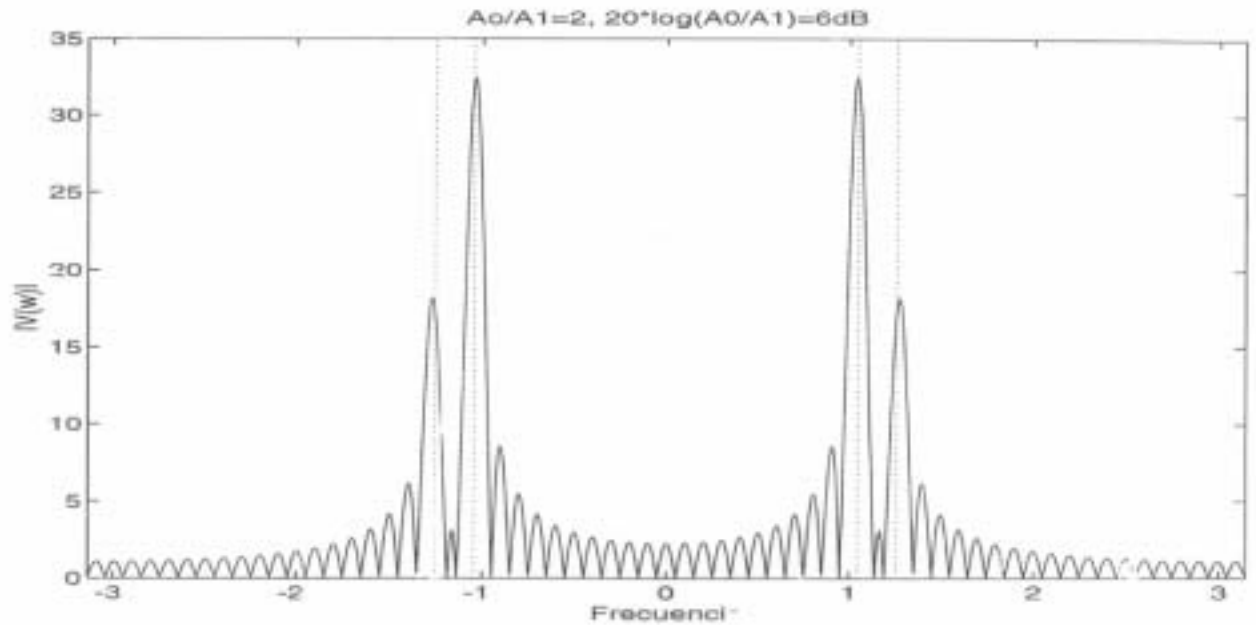


Ventana Rectangular L=8

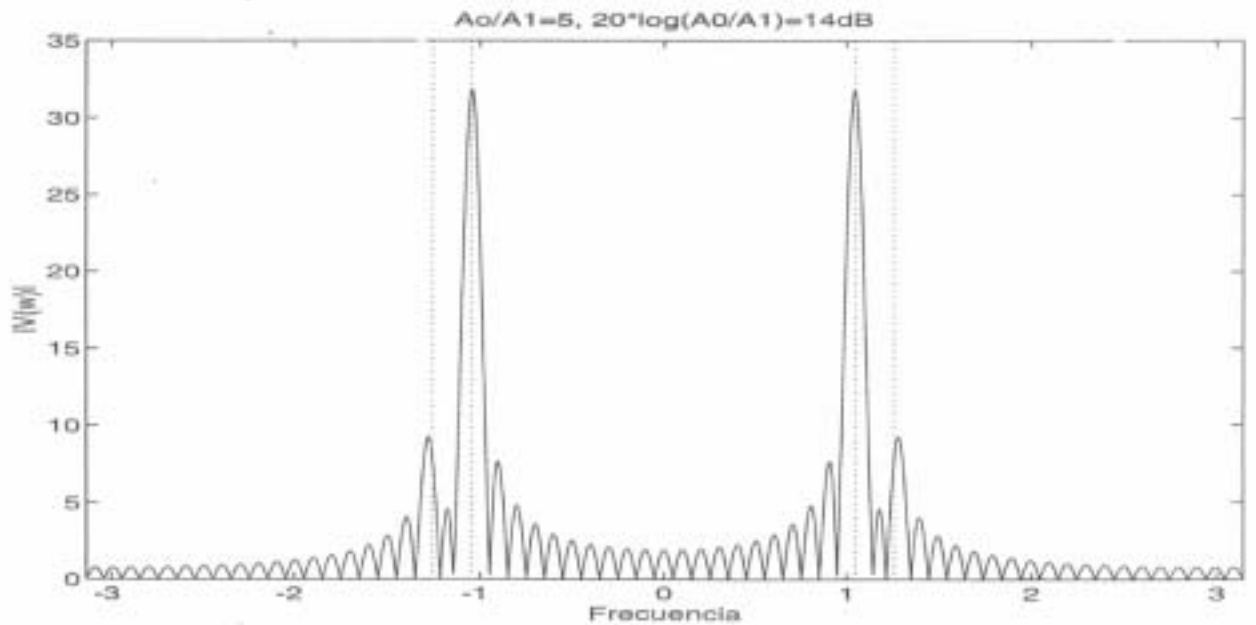
$$|W(e^{j\omega})| = \frac{\text{sen}(\omega L/2)}{\text{sen}(\omega/2)}$$



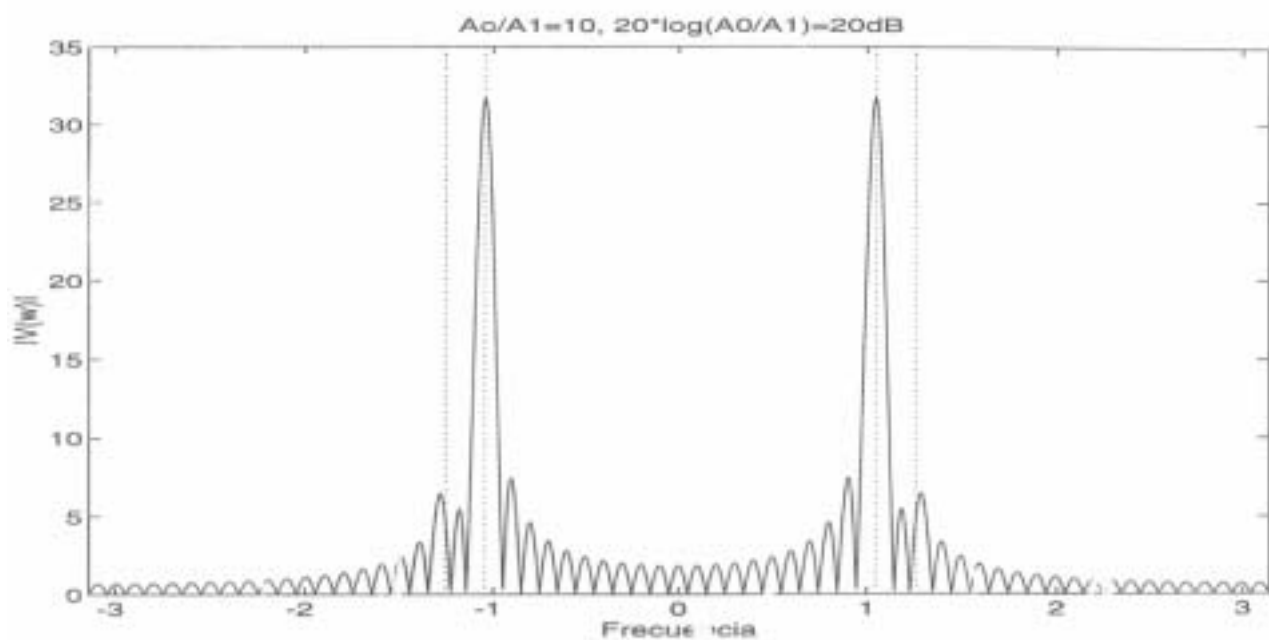
$$\omega_0 = \frac{2\pi}{6} \quad \omega_1 = \frac{2\pi}{5} \quad A_0/A_1 = 2 \quad 20 \log(A_0/A_1) = 6dB$$

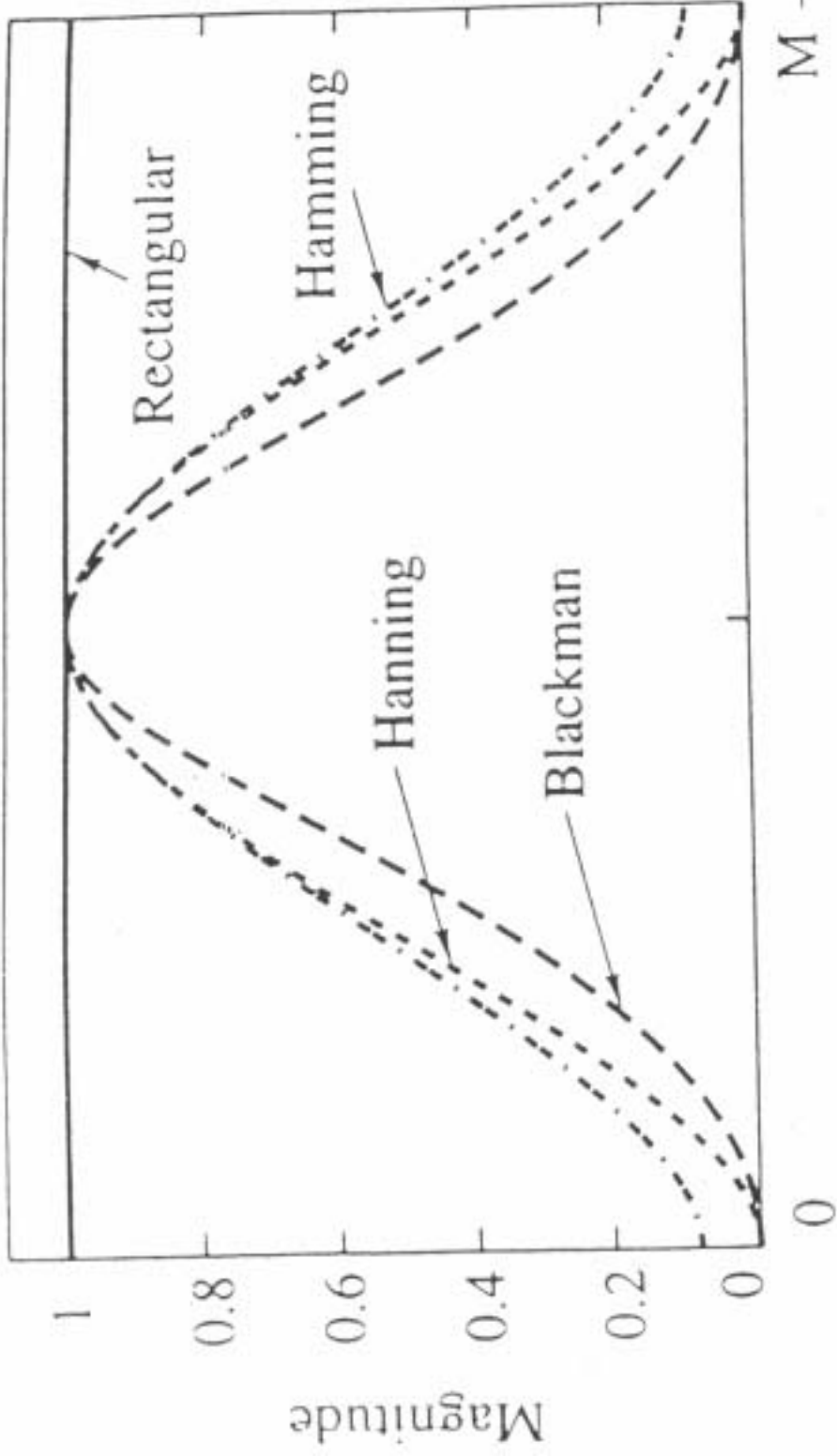


$$\omega_0 = \frac{2\pi}{6} \quad \omega_1 = \frac{2\pi}{5} \quad A_0/A_1 = 5 \quad 20 \log(A_0/A_1) = 14dB$$



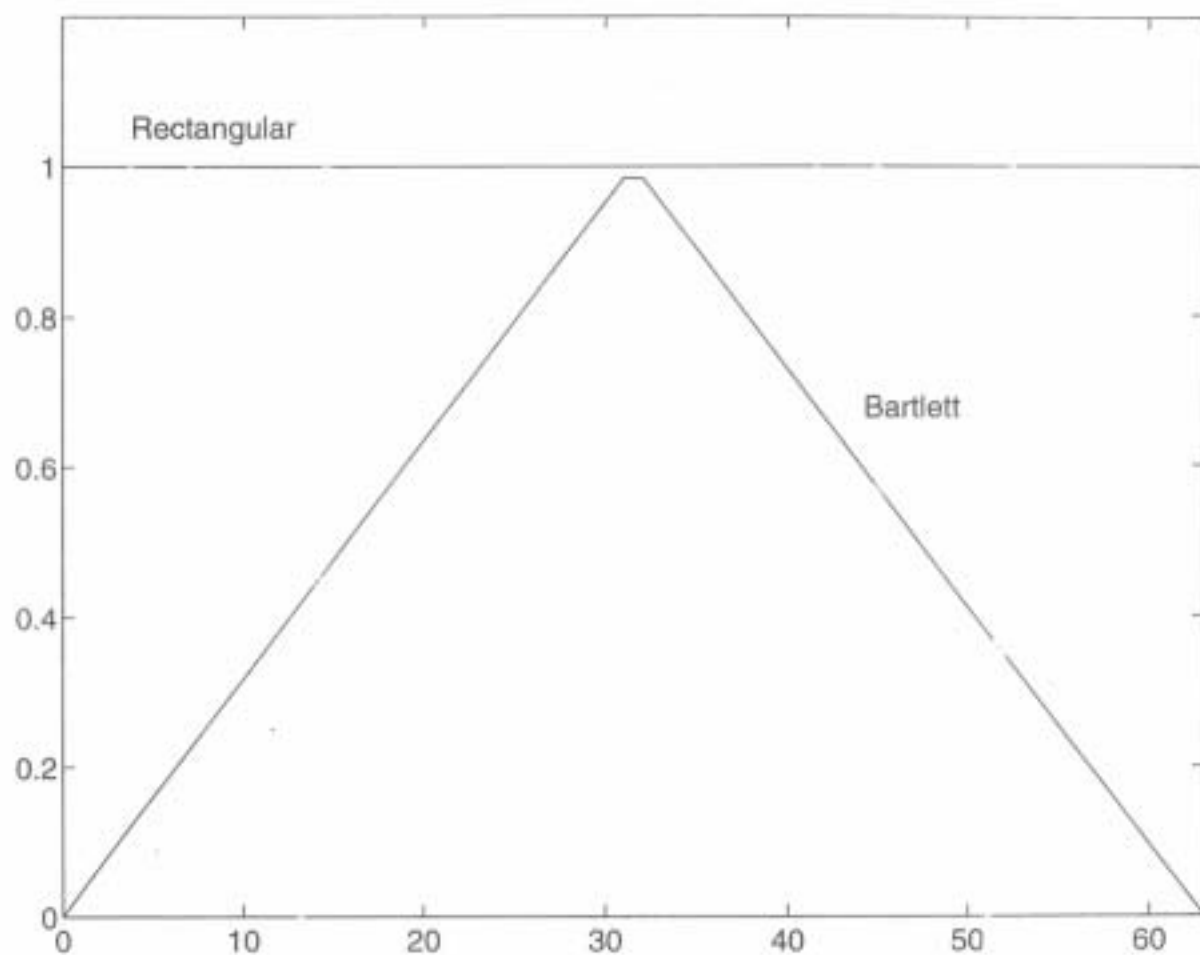
$$\omega_0 = \frac{2\pi}{6} \quad \omega_1 = \frac{2\pi}{5} \quad A_0/A_1 = 10 \quad 20 \log(A_0/A_1) = 20dB$$





Ventana de Bartlett (triangular) L=64

$$w(n) = 1 - \frac{|n - \frac{L-1}{2}|}{L-1}$$



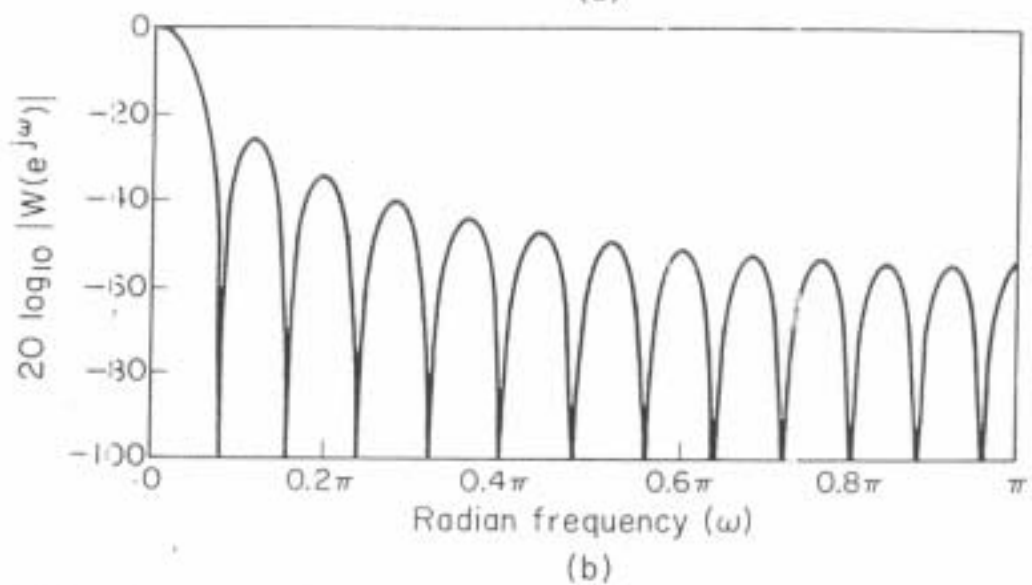
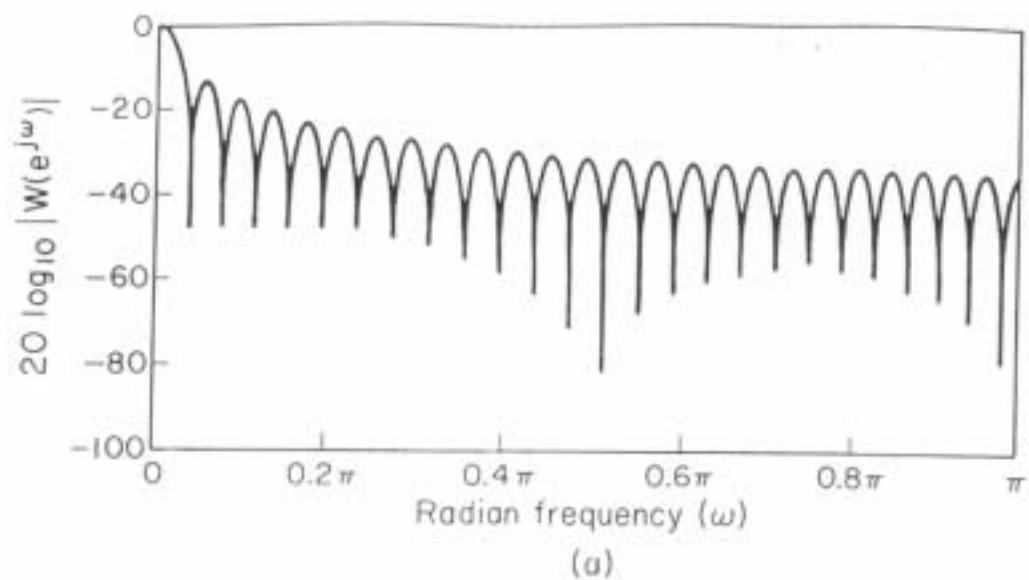
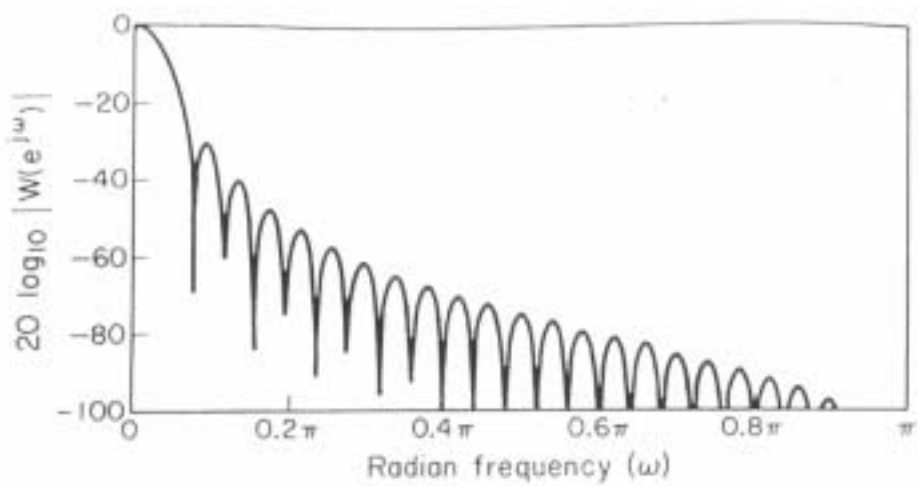
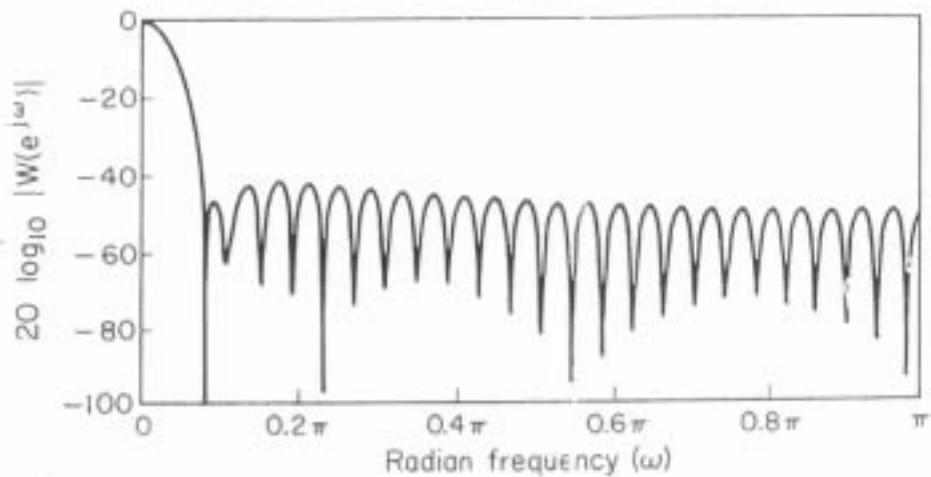


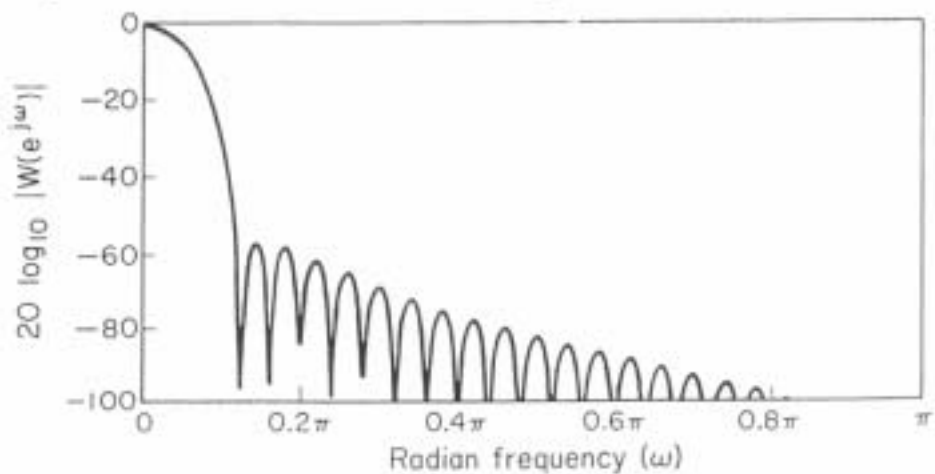
Figure 7.30 Fourier transforms (log magnitude) of windows of Fig. 7.29. (a) Rectangular. (b) Bartlett.



(c)



(d)

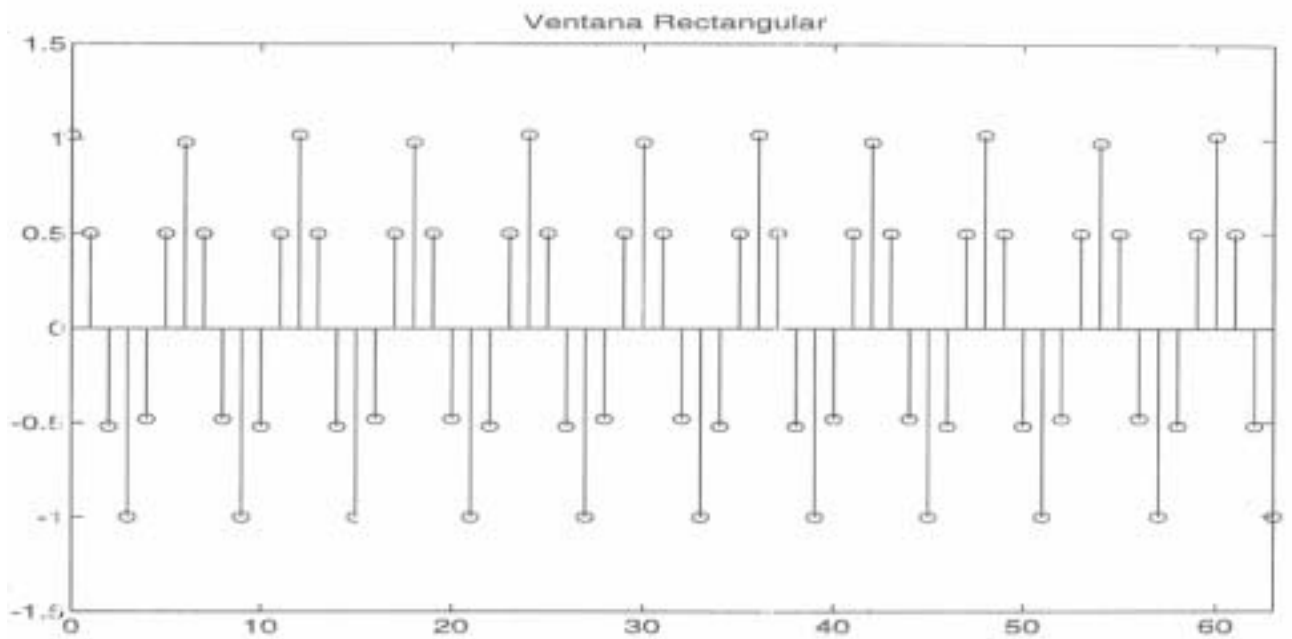


(e)

Figure 7.30 (continued) (c) Hanning. (d) Hamming. (e) Blackman.

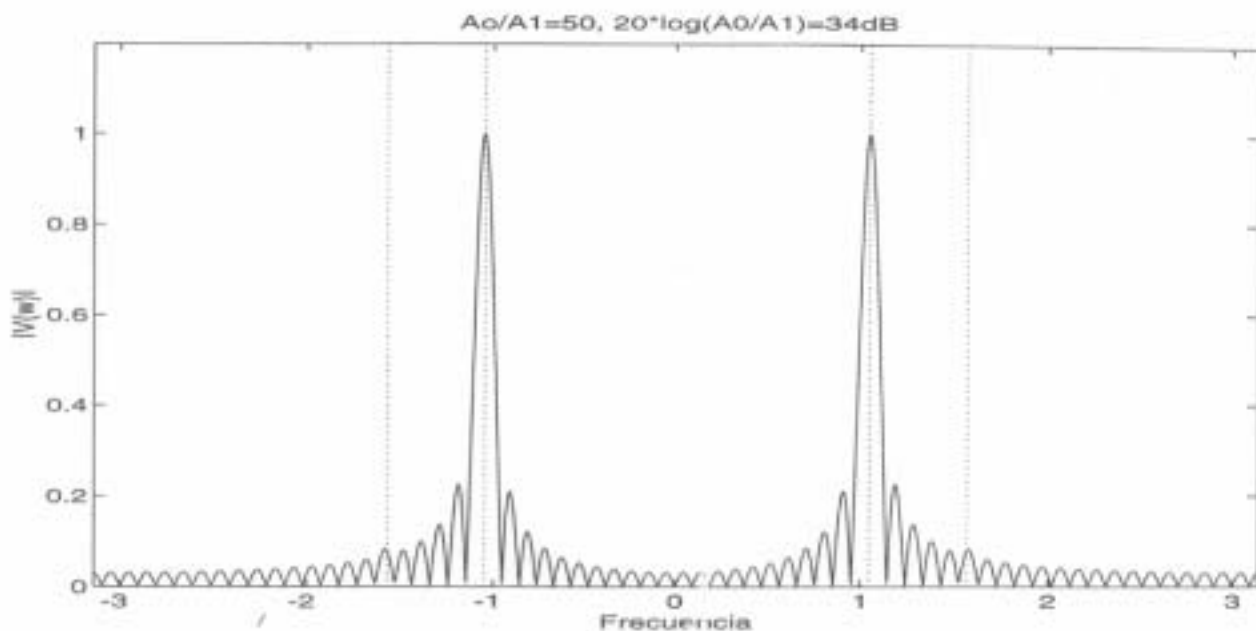
Ventana Rectangular

$$x(n) = \cos\left(\frac{2\pi}{6}n\right) + 0.02\cos\left(\frac{2\pi}{4}n\right)$$

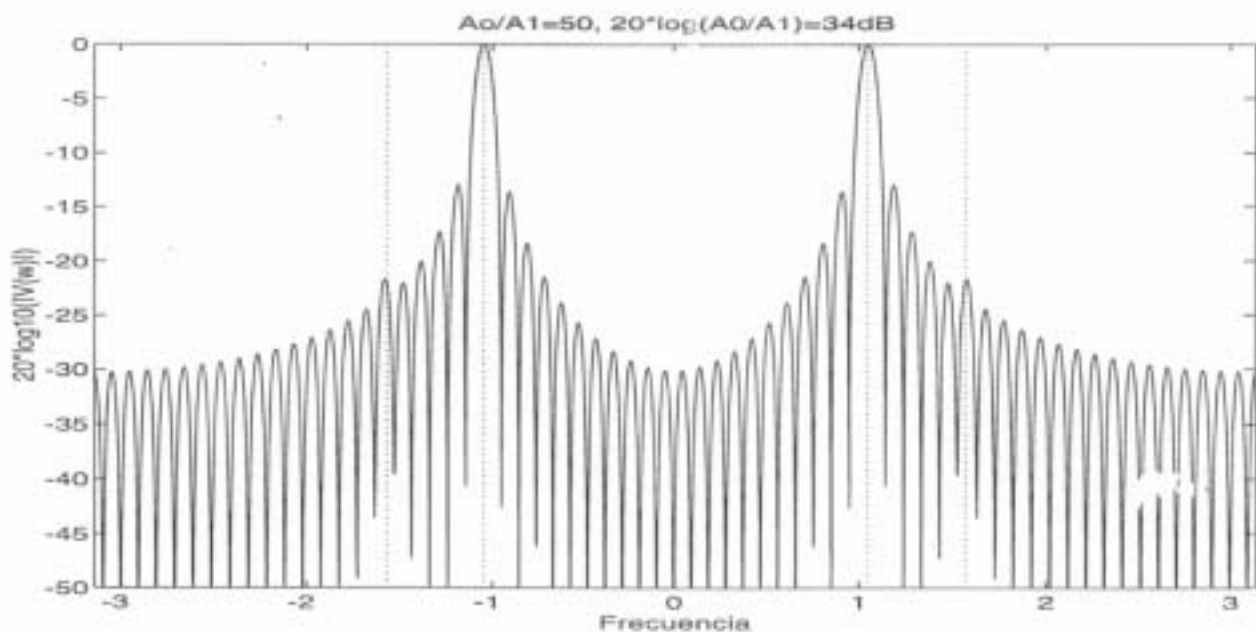


$$A_0/A_1 = 50 \quad 20 \log(A_0/A_1) = 34dB$$

Ventana Rectangular (Escala lineal)

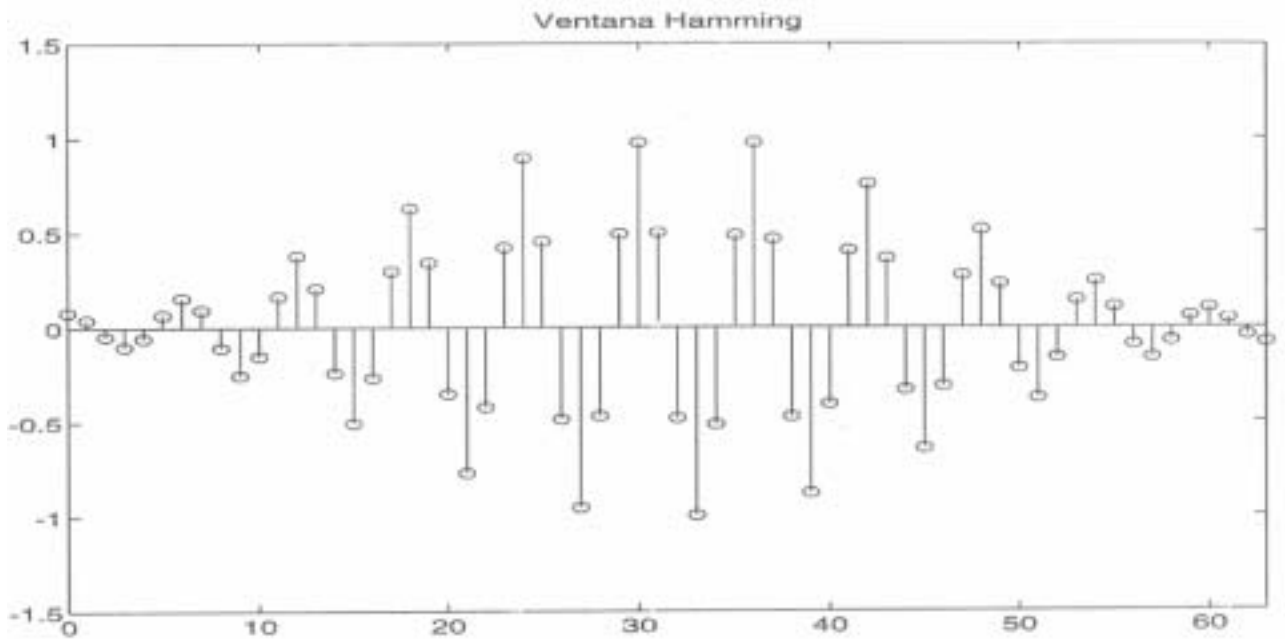


Ventana Rectangular (Escala logarítmica)



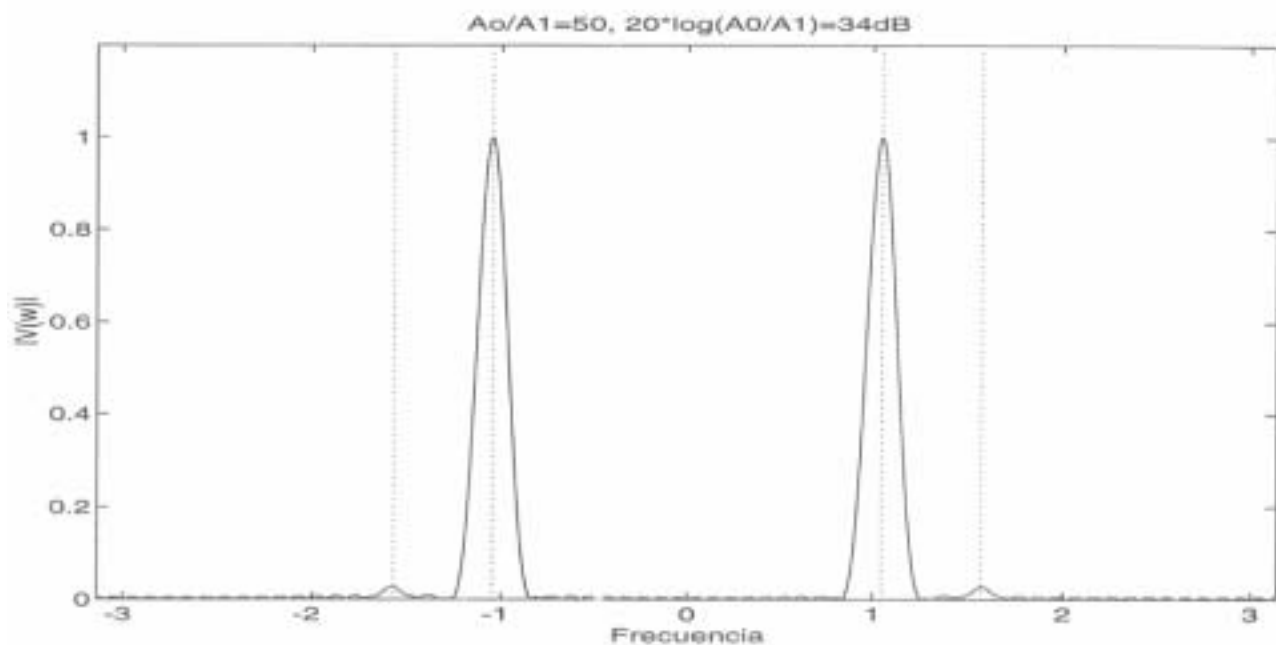
Ventana de Hamming

$$x(n) = \cos\left(\frac{2\pi}{6}n\right) + 0.02\cos\left(\frac{2\pi}{4}n\right)$$

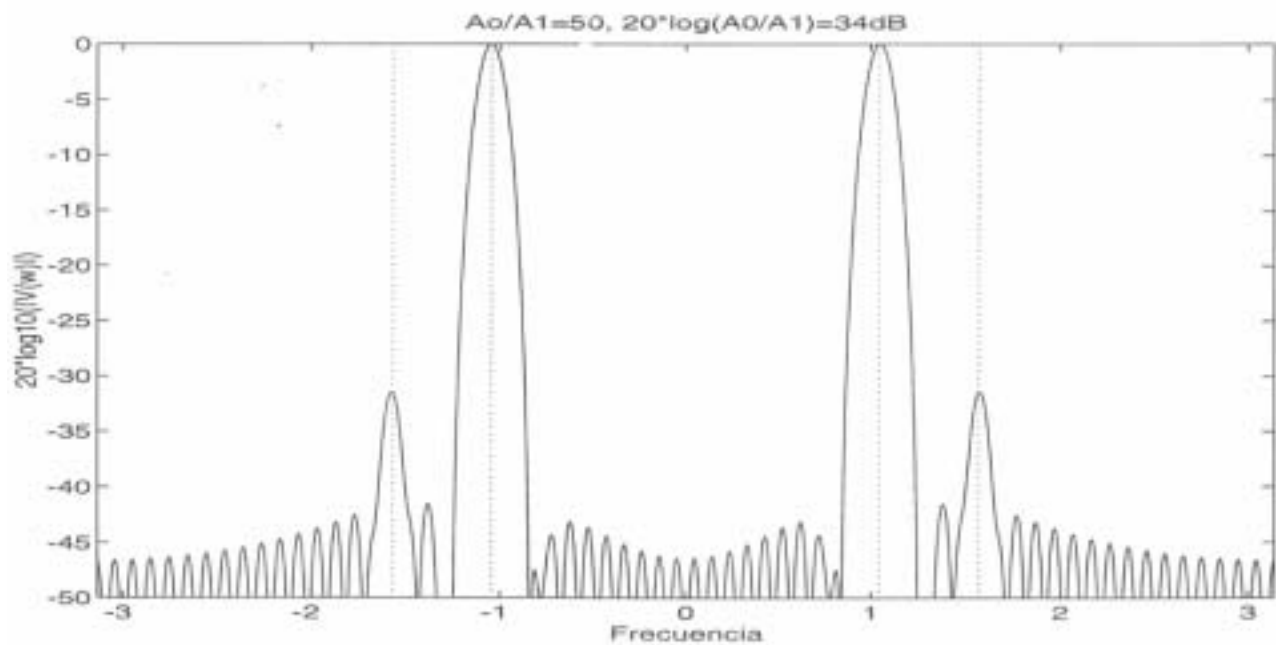


$$A_0/A_1 = 50 \quad 20 \log(A_0/A_1) = 34dB$$

Ventana de Hamming (Escala lineal)

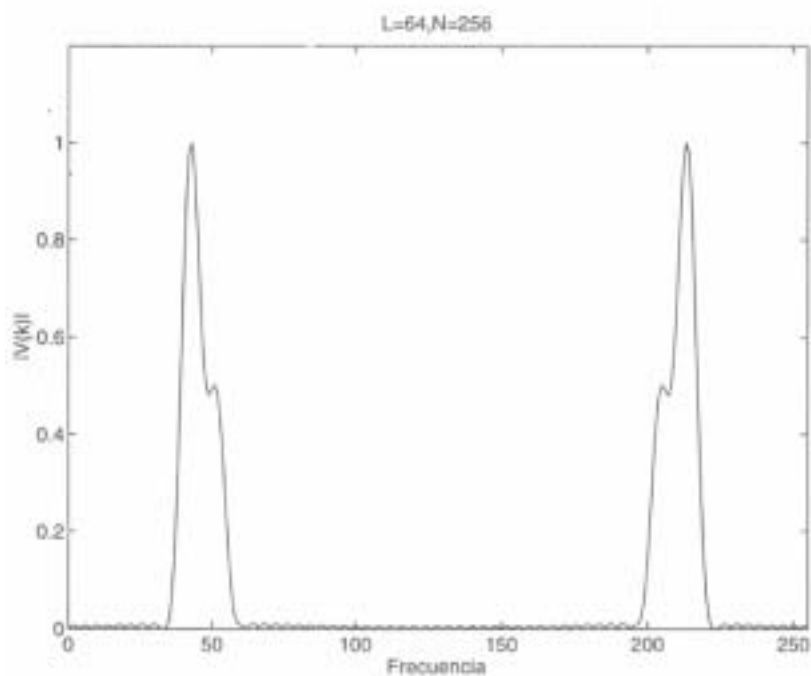
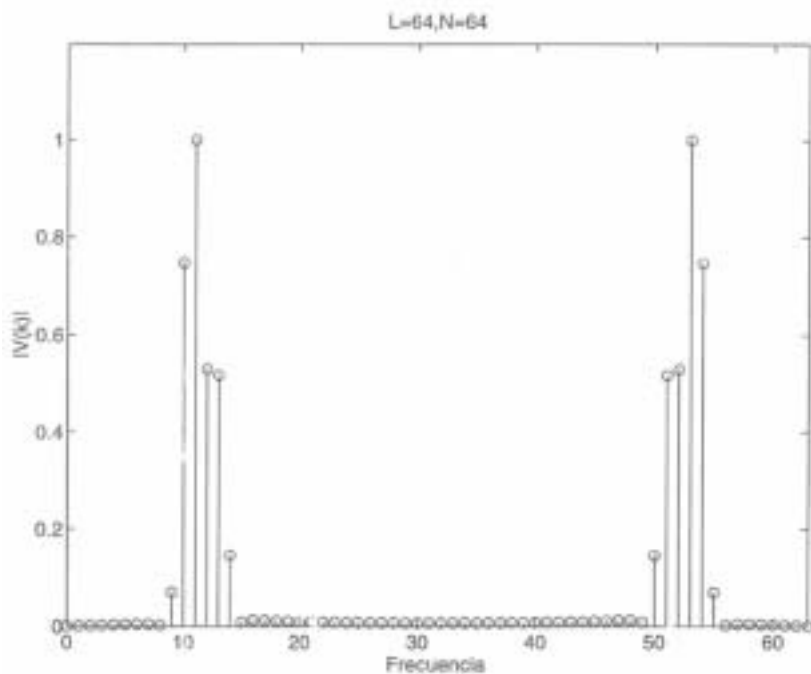


Ventana de Hamming (Escala logarítmica)

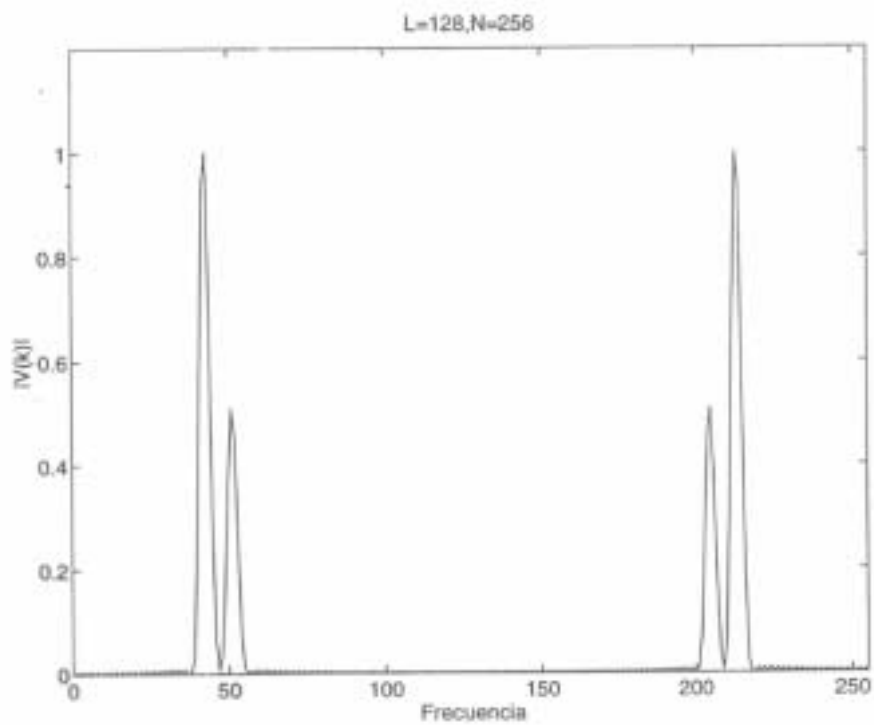
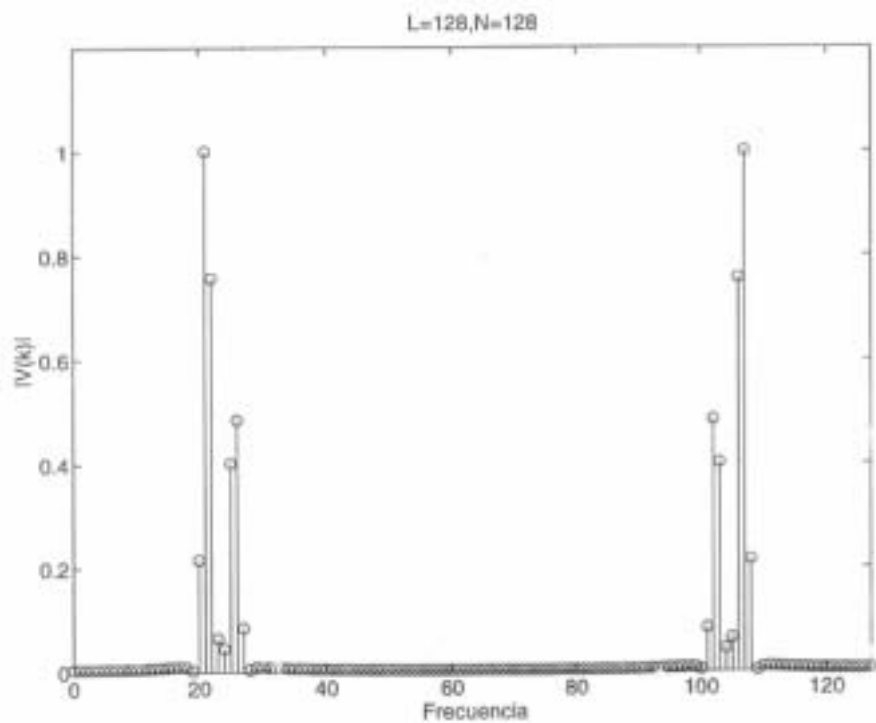


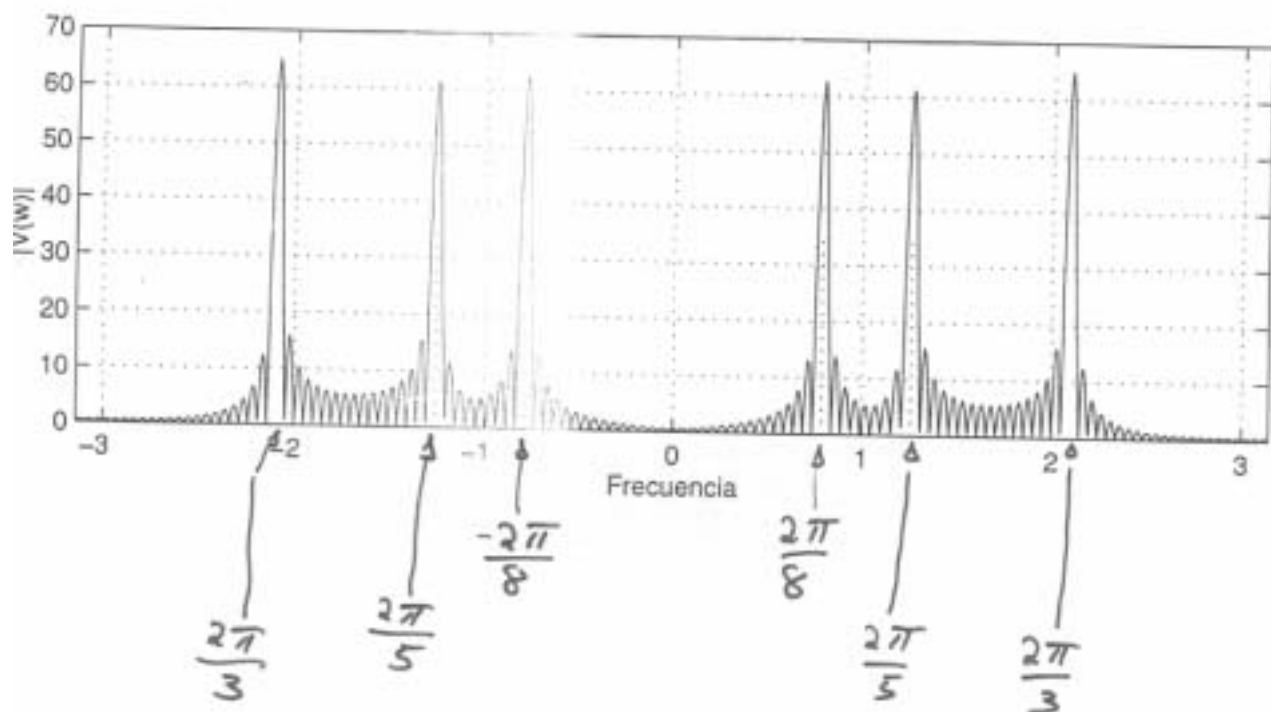
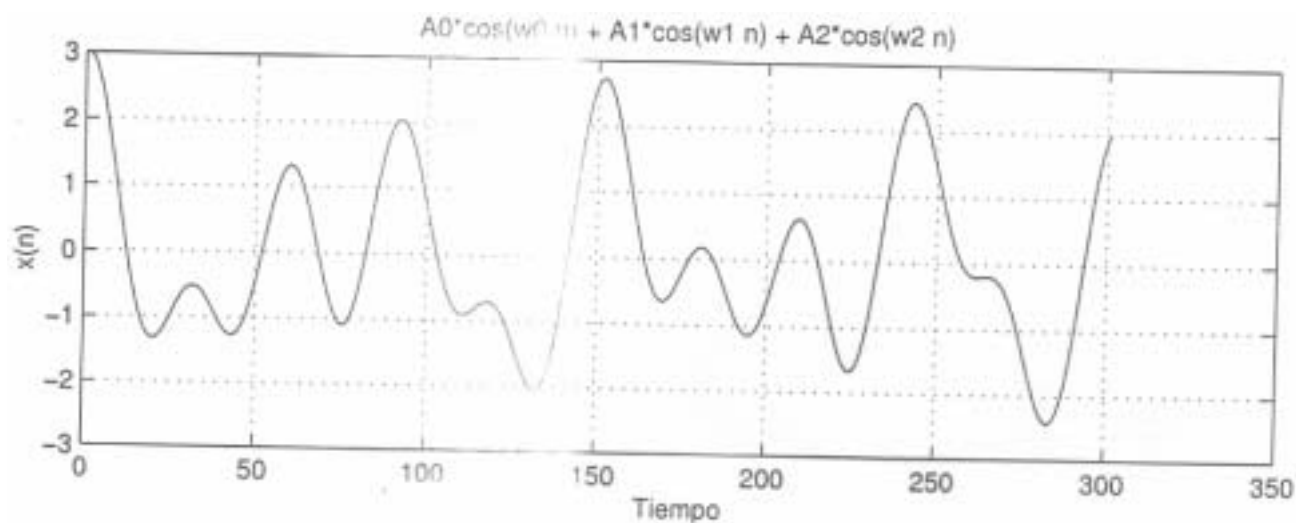
$$x(n) = 0.5 \cos\left(\frac{2\pi}{6}n\right) + \cos\left(\frac{2\pi}{5}n\right), \text{ ventana Hamming}$$

Efecto del muestreo en frecuencia en la DFT



Efecto del muestreo en frecuencia en la DFT





Comparacion operaciones DFT y FFT

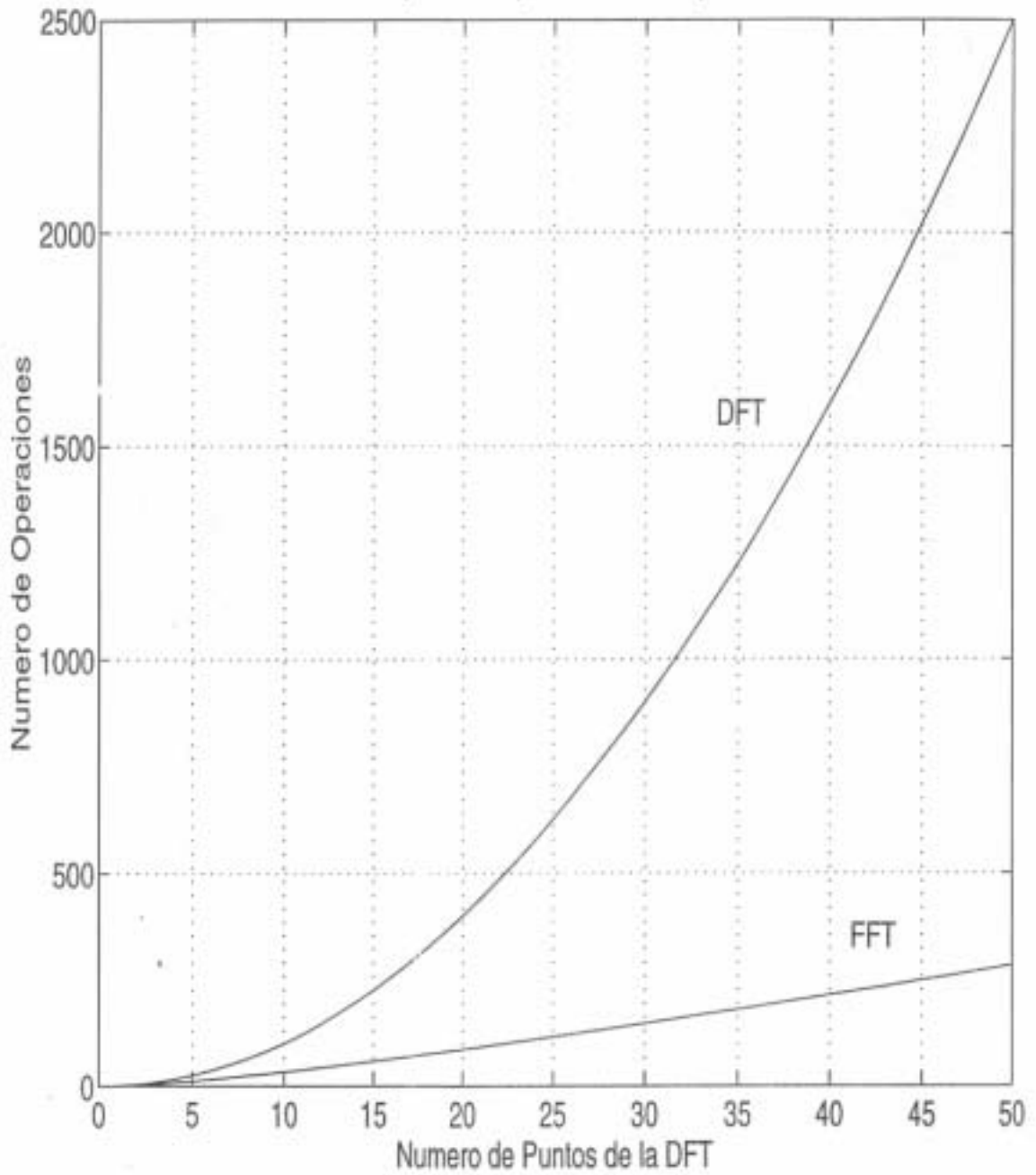


TABLE 6.1 COMPARISON OF COMPUTATIONAL COMPLEXITY FOR THE DIRECT COMPUTATION OF THE DFT VERSUS THE FFT ALGORITHM

Number of Points, N	Complex Multiplications in Direct Computation, N^2	Complex Multiplications in FFT Algorithm, $(N/2) \log_2 N$	Speed Improvement Factor
4	16	4	4.0
8	64	12	5.3
16	256	32	8.0
32	1,024	80	12.8
64	4,096	192	21.3
128	16,384	448	36.6
256	65,536	1,024	64.0
512	262,144	2,304	113.8
1,024	1,048,576	5,120	204.8

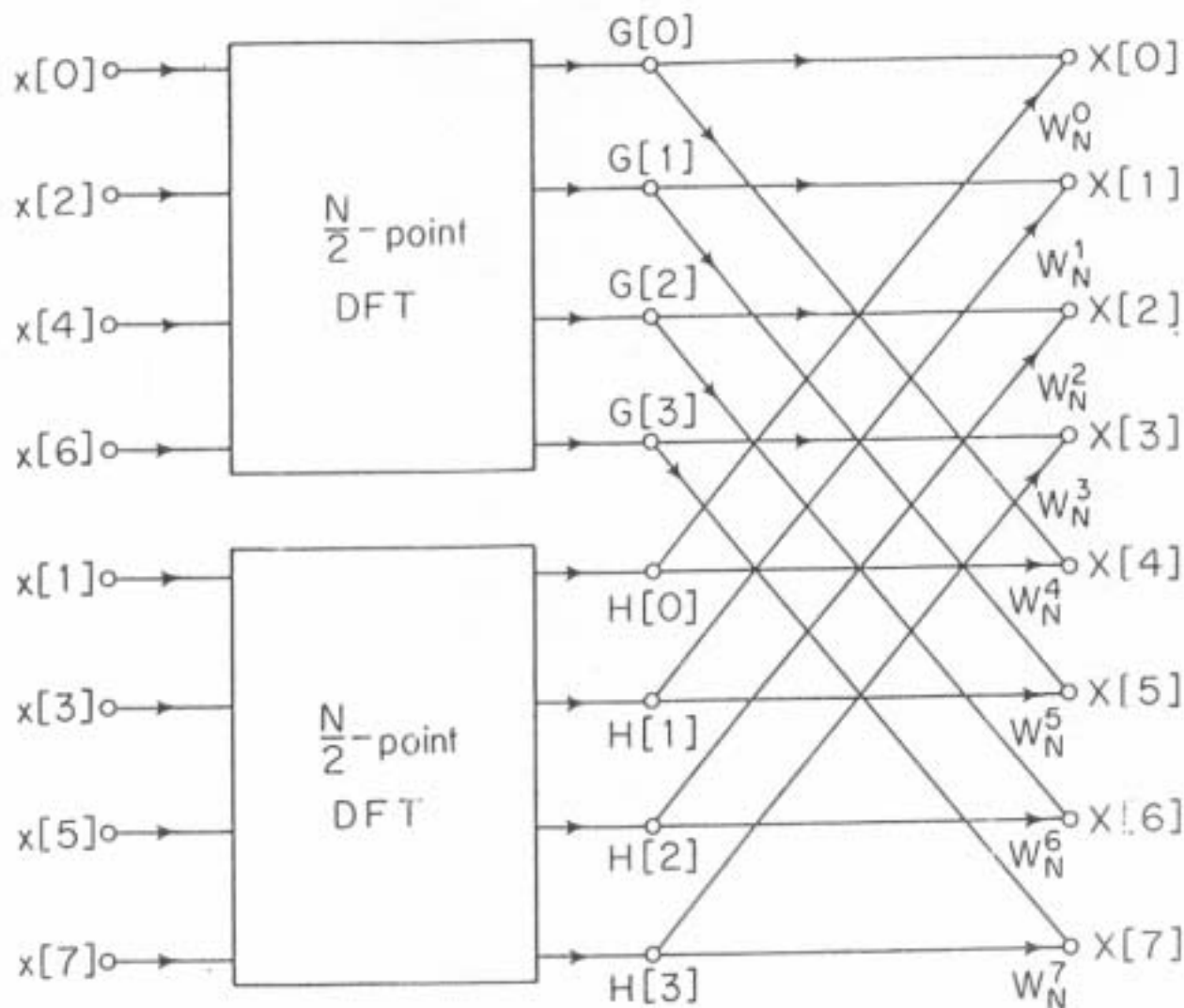


Figure 9.3 Flow graph of the decimation-in-time decomposition of an N -point DFT computation into two $(N/2)$ -point DFT computations ($N = 8$).

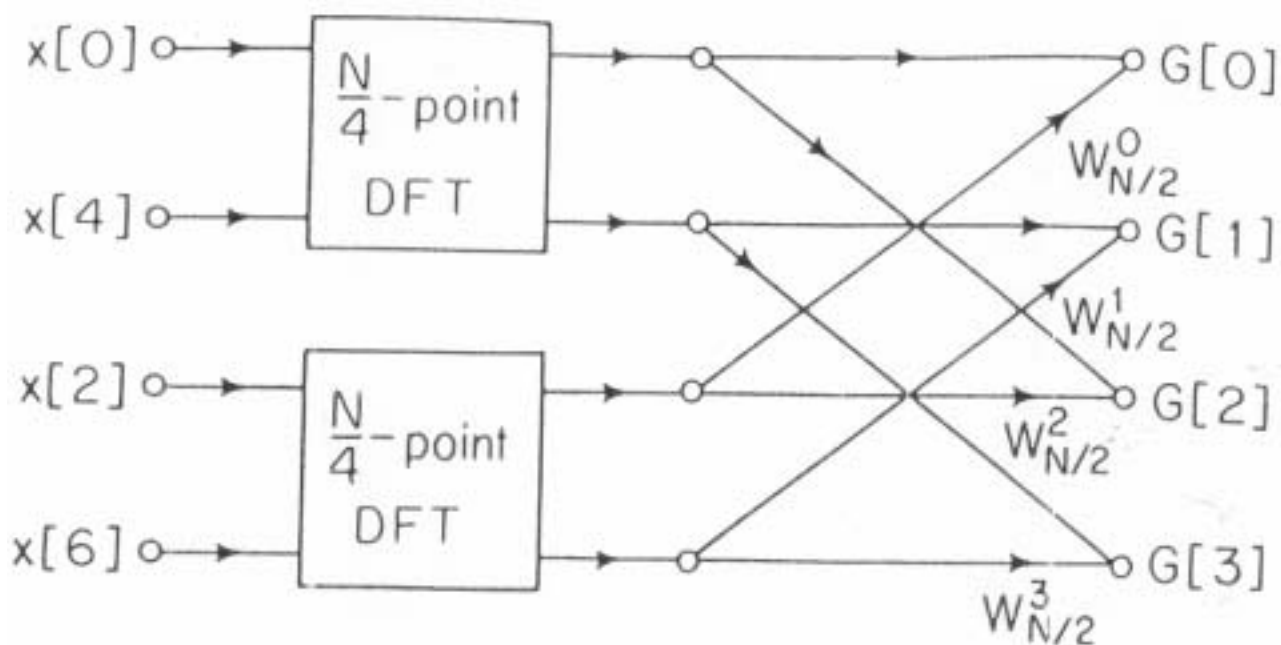


Figure 9.4 Flow graph of the decimation-in-time decomposition of an $(N/2)$ -point DFT computation into two $(N/4)$ -point DFT computations ($N = 8$).

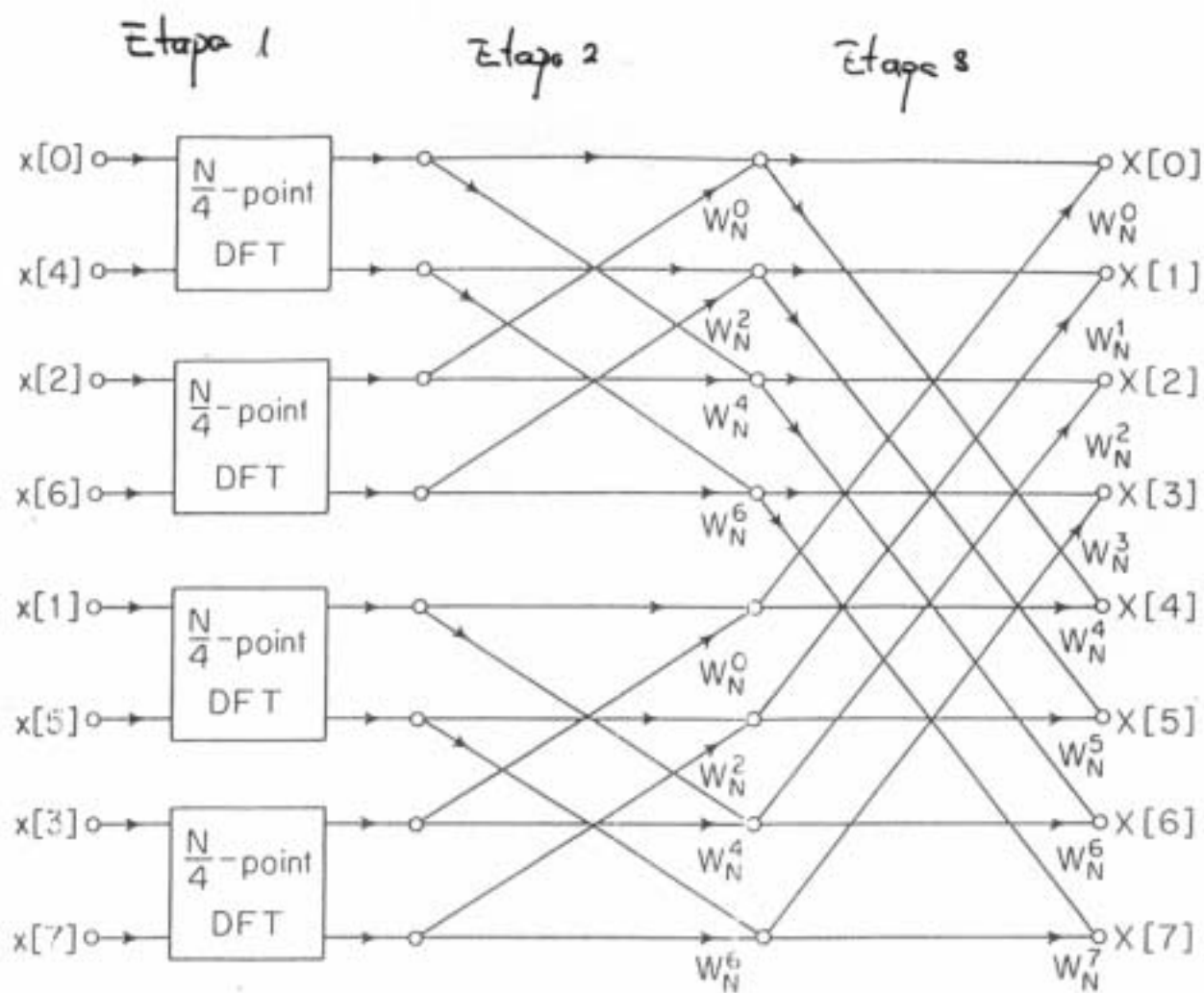


Figure 9.5 Result of substituting Fig. 9.4 into Fig. 9.3.

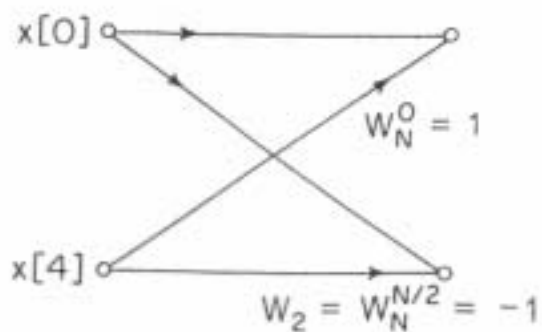


Figure 9.6 Flow graph of a 2-point DFT.

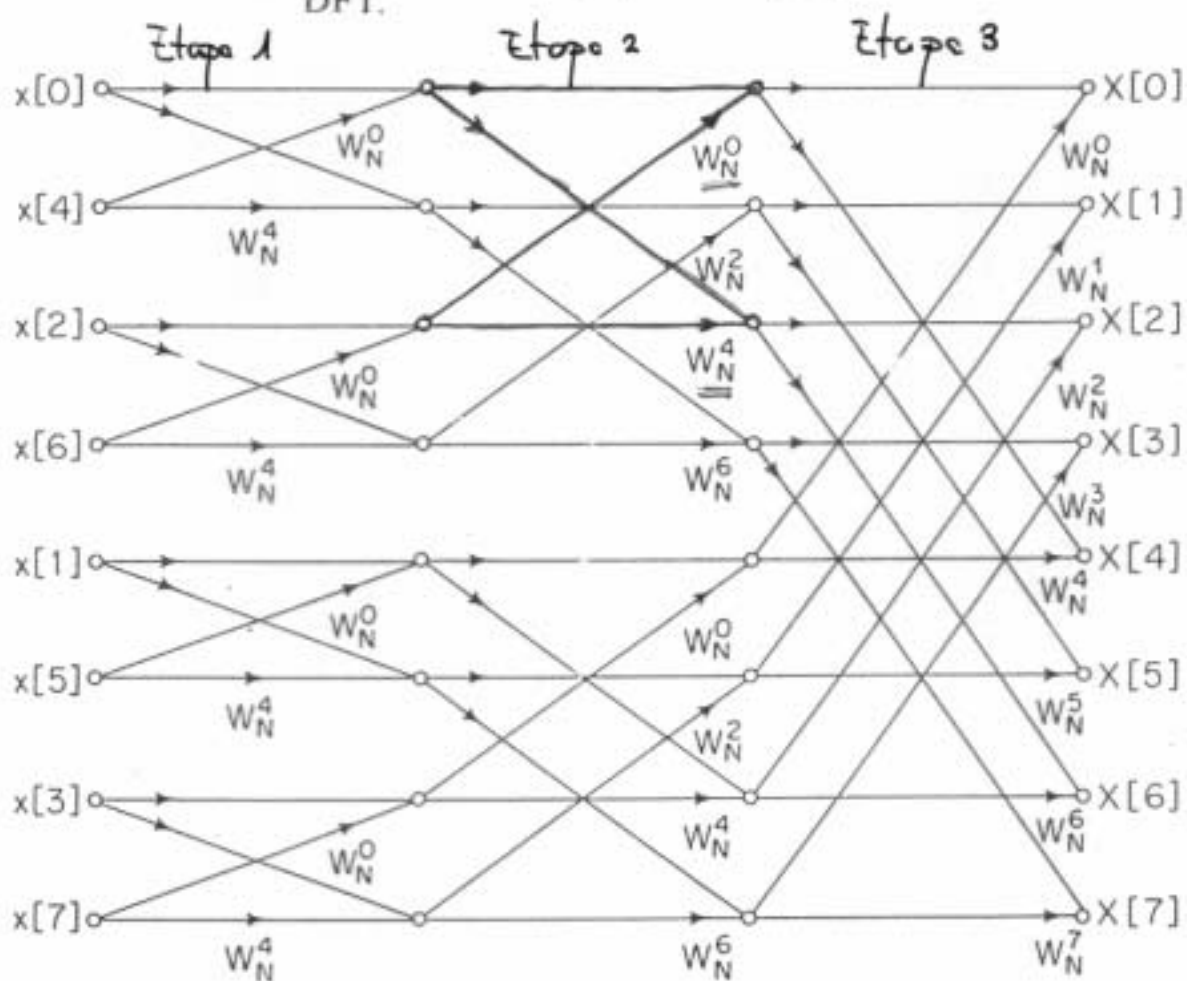


Figure 9.7 Flow graph of complete decimation-in-time decomposition of an 8-point DFT computation.

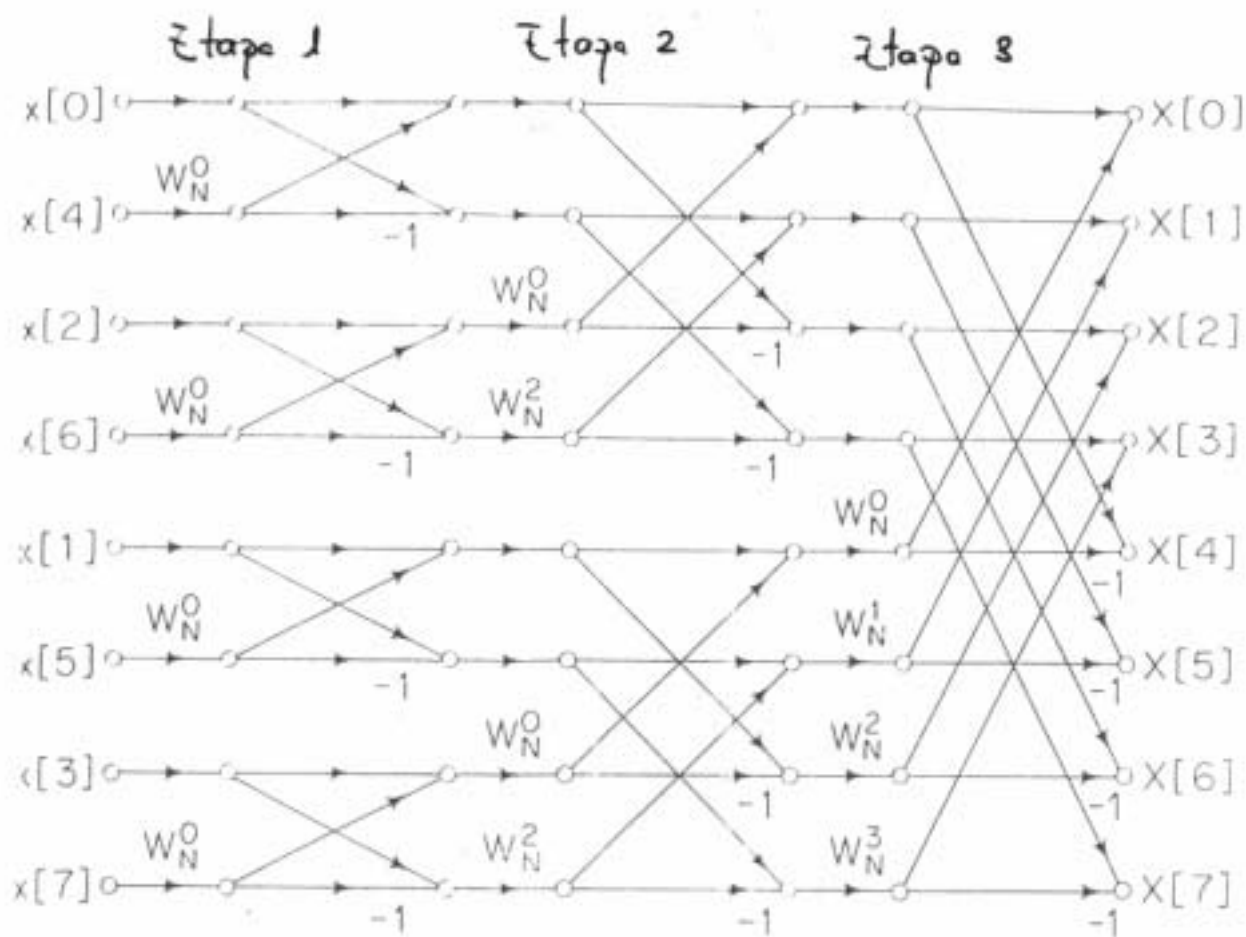


Figure 9.10 Flow graph of 8-point DFT using the butterfly computation of Fig. 9.9.